NANOTECHNOLOGY APPROACH FOR PRECISION TARGETED THERAPY OF OVARIAN CANCER

BY

JUSTIN E. SAPIEZYNSKI

A dissertation submitted to the

School of Graduate Studies

Rutgers, The State University of New Jersey

In partial fulfillment of the requirements

For the degree of

Doctor of Philosophy

Graduate Program in Pharmaceutical Sciences

Written under the direction of

Tamara Minko

And approved by

_____

_____

_____

_____

New Brunswick, New Jersey

October 2019

ABSTRACT OF THE DISSERTATION

NANOTECHNOLOGY APPROACH FOR PRECISION TARGETED THERAPY OF OVARIAN CANCER

BY JUSTIN E. SAPIEZYNSKI

Dissertation Director:

Tamara Minko, PhD.

One of the most pressing health concerns in recent history is cancer. The World Health Organization reports that more than 10 million cases of cancer are diagnosed each year [1]. In the United States, it is the second leading cause of death and is responsible for approximately one in four deaths in the general population [2]. Currently, only about 25% of patients treated with a certain treatment will show a response in the clinic [3]. Therefore, it is necessary to design methods for improvement patient outcomes once being diagnosed with the disease. Precision medicine is a newly found trend in the field of pharmacology to treat patients with more specified treatment regiments for increased efficacy. Patients are further categorized into subtypes based on histology of the disease and new methods are being investigated to further stratify patients based on molecular biology and on the genetic level of the disease in individual patients.

The purpose of the current proposal is to help design precision treatment of ovarian cancer patients. First, we obtained patient biopsy samples from the

Cancer Institute of New Jersey and constructed gene expression profiles to help identify key dysregularities in patients and design an efficient way to screen further patients for these biomarkers. Once gene expression profiles were obtained, we targeted certain overexpressed genes through RNA interference (RNAi) therapy to downregulate their expression in the cancer cells. RNAi therapy was combined with traditional small molecule chemotherapeutics to improve their efficacy compared to being used alone to treat the patients. We categorized and optimized liposomal and dendrimer drug delivery systems (DDSs) to help delivery our proposed combinational therapies. Several small molecule chemotherapeutics were formulated separately with RNAi therapy and evaluated against monotherapies of the corresponding drug. We successfully demonstrated these DDSs efficiently delivered our combinational therapies to tumors, reduced off-site accumulation of the therapeutics, and raised the efficacy of the treatment compared to monotherapies of the corresponding drug.

DEDICATION

To my amazing and wonderful Parents, Jakub and Margaret Sapiezynski,
Who always stood behind me, instilled the importance of knowledge and using it to help others in need.

To my supervisor, Professor Tamara Minko,
Who graciously accepted me into her lab and always gave me a great deal of support and inspiration throughout my studies.

To my beloved wife, Emily Sapiezynski,
Who always stood by my side and always supported me throughout my educational and personal endeavors.

To my amazing son, Lucas Sapiezynski,
Who came into this world one year ago and provided even more purpose to be the best version of myself that I could be in this world.

ACKNOWLEDGEMENTS

First and foremost, I would like to thank God for being with me through the brightest and darkest times of my endeavors.

I would like to thank and express my tremendous gratitude to my supervisor, Dr. Tamara Minko, who has been amazing person and a great source of inspiration throughout my time in her lab. Her patience, support, and valuable suggestions gave me the strength to perceiver to this point and allow me to of my career. I attribute my success in this program to her and all of the encouragement she gave me throughout.

I would like to thank my committee members: Dr. John Colaizzi, Dr. Olga Garbuzenko, and Dr. Guofeng You. All of them were there to help in during the program and even gave me inspiration to make certain decision to my experiments and further my work to this point.

I would like to thank my past lab members and other collaborators to this study: Dr. Andriy Kuzmov, Dr. Oleh Taratula, Dr. Lorna Rodriguez-Rodriguez, Dr. Ronak Savla, and Dr. Millin Shah. These individuals helped contribute to my work, gave me suggestions to improve my study, and showed me how to perform new tasks that I had not previously performed. Without these people, my study would not have turned out the way it did and I own them a great deal of gratitude.

TABLE OF CONTENTS

Contents

LIST OF FIGURES

1 INTRODUCTION

One of the most pressing health concerns in recent history is cancer. The World Health Organization reports that more than 10 million cases of cancer are diagnosed each year [1]. In the United States, it is the second leading cause of death and is responsible for approximately one in four deaths in the general population. Tremendous amounts of effort have been invested into cancer research, resulting in huge improvements to cancer medicine. Since 1991, the rate of mortality due to cancer in the United States has steadily declined by roughly 27% [2]. However, not all types of cancer have been of equal focus to researchers and improvements to treating certain cancers have been less notable.

For instance, ovarian cancer is statically one of the most deadly malignancies for females today. It is the fifth leading cause of cancer-related mortalities worldwide and is the most prevalent gynecologic cancer for women today [4]. There have been considerable amounts of research into understanding the underlying mechanisms ovarian cancer and developing novel treatments, but not nearly as much as other types such as breast cancer. While novel treatments have been approved to treat ovarian cancer over the past few decades, only slight improvements have been made for improving patient outcomes. Only 20% of the patients diagnosed with ovarian cancer are detected at an early stage of the disease and the current 5-year survival rate for patients with advanced-stage

ovarian cancer is a meager 30% [5-7]. Therefore, additional research needs to be conducted on ovarian cancer that can be translated into the clinic.

A recent trend in the field of oncology is the push for precision medicines for treating cancer. Traditional chemotherapeutic agents fail to differentiate between the cancerous cells and normal healthy cells. Since these agents are designed to eliminate tumors by causing cell death, they will kill any cell they interact with inside the body. This indiscriminate destruction can cause damage to healthy non-target tissues and organs, leading to adverse side effects and toxicity issues in patients receiving the treatment [8]. As a result, targeted therapeutics has become one of the main focuses in oncology research to improve the issues with toxicity in patients. Targeted therapeutics exploit abnormalities resulting from disease progression and are not present in healthy cells, tissues and organs [9-11]. Therefore, higher concentrations of the agent will accumulate in the diseased tissues; reducing the amount of off-target accumulation and the prevalence of adverse side effects when treating patients.

Nanoparticle drug delivery systems (DDSs) have demonstrated great potential for precision treatment of cancer. DDSs can improve the PK/PD properties of traditional chemotherapeutic agents by controlling their release in the body [12-16]. Sustained release can be achieved using DDSs and this slower release of the chemotherapeutic agents means that patients could potentially be given fewer doses at high concentrations during their treatment regime [17-19].

However, the ability of DDSs to control the rate in which the agents are released into body is not main reason they demonstrate high potential for precision cancer treatment. It is their capability for cellular targeting that does. By conjugating a certain ligand to a DDS, specifically one that can interact with a cell surface receptor expressed in the diseased states, it acquires the ability to target those cells and produces higher concentrations at the target site of action [20-24]. These ligands are known as targeting moieties and are extremely effective at releasing therapeutic agents precisely at the intended site.

The purpose of this study is to investigate the potential of developing precision combinational therapies for patients with ovarian cancer. The combinational therapy will consist of RNAi and chemotherapy. The two therapeutics will be delivered to the site of action using a DDS. To achieve this, we first established primary tumor isolate cultures from patient biopsies. Once the cultures were established, we established gene expression profiles and determine a set of genes to target for the RNAi therapy. Cationic liposomal and Polypropylenimine (PPI) dendrimers formulations were categorized and the optimal formulations will be used for the combinational therapy. Then we evaluated various combinational therapies against corresponding monotherapies and analyzed the differences in therapeutic efficacy.

2 BACKGOUND AND SIGNIFICANCE

2.1 Ovarian Cancer

As its name suggests, this type of malignancy forms in the female reproductive organ known as the ovaries. Three types of ovarian tissue are known produce cancers (epithelial cells, stromal cells, and germ cells), but the vast majority of ovarian cancers (85 – 90%) occur in the epithelial tissues of the organ [25]. Worldwide statistics reveal it is the seventh most common cancer and the fifth leading cause of cancer-related deaths in women [4, 26]. Additionally, ovarian cancer has been identified as the most prevalent and lethal gynecological as well [2, 27-29].

Oncologists classify ovarian cancer disease progression using four stages. Stage I ovarian cancers are considered to be early cancers since the primary tumor has not begun to metastasize and can only be detected in one or both ovaries. The remaining three stages are considered to be advanced cancers since the primary tumor has undergone metastasis to varying degrees. In Stage II, the primary tumor can be detected in the ovaries and in other areas of the pelvis as well. Stages III ovarian cancers metastasize further and the cancer have spread into areas of the abdomen. By Stage IV, the cancer has spread beyond the abdomen and can be detected in other organs such as the liver, lungs, and lymph nodes [30-32].

Immense amounts of research have been dedicated to uncovering the underlying mechanisms for ovarian cancer progression and discovering novel therapies for treating the disease. While some new therapeutic agents have been approved for treating ovarian cancer over the past few decades, there has been little improvement to the overall survival of patients. Only 20 – 30% of new cases are diagnosed as early stage ovarian cancer since patients tend to be symptomless and reliable diagnostic exams are lacking in the clinic [33, 34]. Symptoms begin to manifest during the advanced stages of ovarian cancer, but therapeutic response in these patients tends to be quite poor and the 5-year survival rate for these patients is approximately 30% [5, 6, 35-37].

Typically, patients with ovarian cancer undergo cytoreductive surgery followed by chemotherapy [37-39]. This therapeutic regime can be effective against early stage ovarian cancers, but becomes frivolous when the disease has progressed to an advanced stage. There are two main reasons for this reduction in treatment efficacy. First, Cytoreductive surgery can only be performed to remove the primary tumor and metastasized cells tend to be unresectable [40]. Additionally, advanced ovarian cancers exhibit high levels of drug resistance to conventional chemotherapeutics [41-44].

2.2 Chemotherapeutics for Ovarian Cancer

2.2.1 Doxorubicin

Doxorubicin (DOX) is a cytotoxic anthracycline antibiotic that was originally isolated from *Streptomyces peucetius* cultures and purified for medical use. The chemical formula for DOX is $C_{27}H_{29}NO_{11}$ with a molecular weight of 543.52 [45-48]. The compound consists of a naphthacenequinone nucleus linked to an amino sugar named daunosamine through a glycosidic bond (Figure 2.1). DOX has multiple mechanisms of action attributing to its cytotoxicity. It can interact with DNA through intercalation leading to the inhibition of specific macromolecule biosynthesis. Additionally, DOX is able to stabilize the topoisomerase II complex formed after it breaks DNA for replication and halts mitosis by preventing the DNA double helix from reforming (Figure 2.2). Last but not least, it has been observed to increase the production of quinone type free radicals [49-52].

It was initially investigated in clinical trials for treating acute leukemia and lymphoma in the 1960's. Since then, it has also received FDA approval for the treatment of other cancers such as bladder, breast, lung, multiple myeloma, ovarian, and thyroid [53, 54]. DOX is generally administered intravenously in the form of a hydrochloride salt and formulations either contain the free drug or an encapsulated form of the drug. Formulations containing the free salt form of the drug are sold under the brand names Adriamycin and Rubex [55, 56]. Liposome-encapsulated DOX is sold under the brand name Doxil. Doxil is primarily for the

treatment of ovarian cancer in patients who have already undergone platinum-based chemotherapy and have observable disease recurrence [57, 58].

2.2.2 Paclitaxel

Paclitaxel (PTX) is a mitotic inhibitor that is commonly used to treat many forms of cancer. The compound was discovered in bark extracts of the Pacific yew tree, *Taxus brevifolia*, in 1971 by Wani and colleagues [59]. It was later discovered that it was not the tree that produced the compound, but an endophytic fungus that grows within the bark of the tree [60, 61]. The chemical formula for PTX is $C_{47}H_{51}NO_{14}$ with a molecular weight of 853.91 [62]. PTX is a tetracyclic diterpenoid (Figure 2.3). The mechanism of action of PTX is that it interacts with microtubules within the cell. The compound binds to the β subunit of tubulin in a highly selective manner and this causes the formation of highly stable microtubules that resist the depolymerization process catalyzed by calcium molecules. The conversion of microtubules to tubulin dimers is extremely important process during cell division. PTX therefore inhibits spindle formation, causing disorganized microtubules within the cell, and ultimately causes cell cycle arrest (Figure 2.4). Eventually the stress caused by the cell cycle arrest and causes the cells to undergo apoptosis [63-65].

In combination with platinum-based chemotherapeutics, PTX is typically apart of first-line therapy regimes for the treatment of ovarian cancer [66-71]. It can be a

highly effective therapeutic agent, but the hydrophobic nature of the compound limits its efficacy. Since it has extremely poor water solubility, PTX is usually formulated with co-solvents for intravenous administration. Cremophor EL or similar co-solvents are administered with PTX to improve the solubility issue, but these can cause anaphylaxis in patients. Additionally, Cremophor EL exhibits both neuro- and nephrotoxicity [72-74]. This factor unfortunately limits PTX dosing and ultimately treatment efficacy in patients. A new strategy for overcoming this limitation is developing encapsulated PTX formulations. Abraxane is the name brand for albumin-bound PTX currently FDA approved for the treatment of metastatic breast, non-small cell lung cancer, and pancreatic adenocarcinoma [75, 76].

2.2.3 Cisplatin

Cisplatin (CIS) is a platinum-based chemotherapeutic drug that is FDA approved for the treatment of many types of cancers including breast, lymphoma, ovarian, sarcoma, and small cell lung cancer [77]. Discovered in the mid-19th century, CIS was the first therapeutic developed in the platinum-based drug class. It underwent clinical trials in the 1970's and received FDA approval shortly after in 1978 [78-81]. The chemical formula of CIS is $Pt(NH_3)_2Cl_2$ with a molecular weight of 300.05 [82]. The compound consists of a platinum nucleus bound with two ammonia groups and two chlorine atoms (Figure 2.5). It is water-soluble and typically formulated to be administered intravenously [83]. CIS has a mechanism

of action that interacts with DNA and ultimately causes apoptosis. Once administered, it interacts with the aqueous environment of the body and hydroxyl groups replace the chlorine atoms. The hydroxyl groups then interact with DNA, binding to it, and cause crosslinking (Figure 2.6). Signals are produced through the crosslinking that activate DNA repair mechanisms, which ultimately fail and trigger the cell to undergo apoptosis [84, 85].

There are a few limitations of CIS that cause reduced efficacy in patients. First, it is known to cause a wide array of side effect in patients. Side effects observed in patients undergoing a therapeutic regime with CIS include alopecia, electrolyte imbalance, leukopenia, myelosuppression, nephrotoxicity, neurotoxicity, ototoxicity, severe nausea, and excessive vomiting [82, 86, 87]. Second, CIS-resistance has been observed in disease progression and in patients diagnosed with advanced-stage cancers [52, 86]. The mechanisms proposed for CIS-resistance in cancer cells include reduced cellular uptake, increased cellular efflux, increased detoxification/metabolism of CIS, inhibition of apoptosis, and increased levels of DNA repair mechanisms [88]. These two factors have led investigators into developing strategies for targeted delivery of CIS to the intended site of action, in order to reduce off-target side effects, and for overcoming CIS-resistance [87, 89-91].

2.3 Precision Cancer Medicine

The field of oncology is an area of medical care that is constantly undergoing changes due to massive investments into investigating the disease. New developments are continually uncovered in various fields of research, leading to improved patient care in the clinic. One major aspect of the disease researchers emphasize is the extreme complexity and high variability it can have in different patients [92-94]. Not only has this shaped oncologists view different types of cancers originating in different organs, but also between patients of the same type of cancer and this has led to patients being further stratified into different subtypes of the disease [95-98]. As a result, precision cancer medicine is now a major focus to researchers.

Precision medicines are developed through understanding the underlying mechanisms that cause a disease. In the field of oncology, they integrate genetic and biochemical data on patient populations in order to develop therapeutic agents that focus on disease-specific targets.

2.3.1 Cellular Dysregulation

Mutations in the genome can lead to the development of mutated proteins that exhibit different properties than the wild-type protein such as their activity and turnover rate [99-101]. Moreover, dysregulation in transcription can be caused by

mutations to the genome and in specific proteins. In eukaryotes, different regulatory proteins control gene expression. These proteins bind gene-specific sequences such as enhancers and silencers that alter the levels of transcription [102-104]. Mutations in these proteins or regulatory sequences can alter their affinity for binding, leading to abnormal transcription activity for certain genes. It has been well documented that mutations in the p53 protein's DNA-binding motif can cause it to be unable to bind certain enhancer sequences. More importantly, one of the genes induced by p53 is a cell cycle regulatory protein that prevents the cell from entering M phase. Ultimately, this mutation leads to an uncontrolled checkpoint in the cell cycle and has been known to cause neoplasm formation [99, 105].

2.3.2 Identifying Disease-Specific Therapeutic Targets

Conventional chemotherapeutics are known to not only be cytotoxic to cancer cells, but healthy cells as well and this limits their efficacy in the clinic. Therefore, developing therapies that target disease-specific biomarkers would increase therapeutic accumulation at the tumor site and reduce off-site cytotoxicity.

In order for oncologists to decide which therapeutic strategy on a patient will be optimal, they need to perform diagnostics that will help them identify biomarkers present in the patient. Molecular profiling patient biopsies can help uncover genomic mutations, dysregulation patterns in transcription, and altered protein

activities present in the tumor [106-110]. Since such changes are able to produce changes in cellular physiology and the unregulated growth observed in cancer, they can possibly identify novel disease-specific targets for precision therapies.

Genomic sequencing a specific patient population is one way to achieve this goal. Since the human genome project was completed, researchers have been able to identify relationships between many diseases and corresponding mutations in the genome [111-114]. It has been known for decades that certain inherited mutations in a family line can make individuals more susceptible to developing certain cancers. One of the most notorious examples of this is the relationship between inherited BRCA1/2 mutations and breast cancer. However, inherited mutations are detected in a small fraction of the overall cases of ovarian cancer diagnosed. A recent study concluded that out of the 21,290 cases of ovarian cancer diagnosed in 2015, only 10 – 15% of patients had known germline mutations [115-117]. Most patients develop ovarian cancer when they have become post-menopausal and it is believed that sudden shifts in hormone levels may lead to sporadic mutations that contribute to neoplasm formation [118-120]. As a result, genomic sequencing could be a useful tool for identifying novel disease-specific targets in ovarian cancer patients.

Transcriptome profiling to identify gene expression patterns in cancer patients can be very useful for developing precision therapies. Genetic dysregulation is the basis for cancer development and progression. Analyzing transcriptome

profiles can help oncologists better understand the underlying mechanisms causing the disease in patient populations and even in individuals. This could further stratify patients on a molecular level for more detailed disease subtypes. Subtype-specific gene signatures have been shown to help predict treatment response, tumor progression, and even patient prognosis [121-125]. One method for obtaining patient transcriptome profiles is quantitative reverse transcription polymerase chain reaction (qRT-PCR). Another popular method is microarray analysis. Both methods require isolating total RNA from samples; reverse transcribing the RNA into complementary DNA (cDNA), quantifying the cDNA in the samples, and comparing gene copy numbers to control samples [126, 127].

2.3.3 Cell-Specific Targeting Moieties

Another concept that has been gaining popularity recently is targeted delivery of conventional chemotherapeutics specifically to cancer cells. By exploiting overexpressed cell surface receptors, it is possible to increase the accumulation of chemotherapeutics at the desired site of action. Ligands that interact with the overexpressed receptors can be conjugated to a drug and have been shown to increase its delivery and internalization of specific cells [9, 128-132]. Aside from ligands, targeting moieties can also be antibodies and proteins as well [133].

Luteinizing hormone-releasing hormone (LHRH) peptide has been discovered to be a great candidate for targeting cancer cells. Investigations demonstrate that

LHRH receptors are expressed in roughly 80% of ovarian cancer patients [134]. Previous work in different labs has identified the LHRH receptor is highly expressed by several types of cancer cells such as breast, ovarian, and prostate. More importantly, LHRH receptor expression in healthy cells and visceral organ is virtually undetectable [135-137]. Consequently it is not the perfect candidate for all patients with ovarian cancer, but years of research has already proven there is no “one size fits all” answer for cancer treatment.

There are many advantages to utilizing LHRH as a targeting moiety to treat ovarian cancer. First, the interactions between LHRH and its receptor can help improve the rate of internalization of chemotherapeutics into cancer cells. Free chemotherapeutic small molecule drugs are typically internalized into cells by simple diffusion. Once they are inside the cells, these drugs can be easily removed from the cell by efflux transporter proteins such as MDR-1 [44, 138, 139]. The mechanism of LHRH-mediated cellular internalization is endocytosis. A vesicle is formed around the DDS, which can protect chemotherapeutics from immediate efflux. Emons and his team demonstrated this by conjugating LHRH to DOX (Figure 2.7). Once the DDS is internalized, the protective vesicle migrates towards the nucleus, and eventually releases the drug to exhibit its cytotoxic effects on the cell [140]. Zhang and team further validated this concept by investigating liposomal DDS formulations. Liposomes encapsulated DOX or CIS and were formulated with and without LHRH. The liposomes without LHRH-mediated cell targeting accumulated equally in the tumor and other organs such

as the liver and kidneys. This is a similar distribution demonstrated by free drug administration. However, the LHRH targeted liposomes accumulated primarily in the tumor and only trace amounts were detected in other organs [141]. Thus, LHRH-mediated cell targeting can improve the efficacy of conventional chemotherapeutics and reduce toxic side effects observed in patients when treated with the free drug.

2.4 RNA Interference (RNAi) Therapy

RNA interference (RNAi) is a technique originally utilized by molecular biologists to study the functions of various genes. It was discovered that certain viruses have RNA-based genomes and that eukaryotic cells have mechanisms to detect the double stranded viral RNA and degrade it before integrating into the host genome [142, 143]. As a result, molecular biologists took the concept and injected gene-specific sequences of double stranded RNA (dsRNA) into various organisms and noticed it silenced the corresponding gene's expression by degrading the mRNA prior to protein translation. Since the protein is never synthesized, the functions it would normally perform do not occur and it is essentially as if the gene expression never occurred. The mechanism for RNAi is a two-step process (Figure 2.8). When the cell detects dsRNA (typically greater than 200 base pairs), RNase III family nuclease (Dicer) cleaves it into smaller strands, referred to as short interfering RNA (siRNA), roughly 20 – 25 base pairs [144]. A multi-enzyme complex, comprised of the RNA-induced silencing

complex (RISC) and Argonaute 2 (AGO2), recognizes the smaller strands. The complex separates the two RNA strands, cleaves the sense strand, and retains the antisense strand. Retention of the antisense strand allows the complex to target mRNA, which bear the complementary sequence and cleave it before it can be translated [145-147].

Fire and team first executed the technique in 1998 when they injected dsRNA in *Caenorhabditis elegans* cells and confirmed gene silencing occurred as a result [148]. Molecular biologists further investigated the technique in other organisms to study specific gene functions and their effects on cellular physiology and organism development/maturation [149-153]. In 2001, Elbasir and team published a study that provided evidence that siRNA can be successfully used in mammalian cells to silence specific genes [154]. Injecting siRNA into cells meant the first step in the RNAi mechanism could be bypassed. This is important because early research into RNAi discovered that dsRNA cleaved into strands longer than 30 base pairs would activate interferon response and resulted in non-specific gene silencing [155]. The discovery of siRNA meant gene silencing could be extremely precise and sparked a lot of interest into further researching new pathways for gene silencing. Ultimately, this led to revolutionizing our understanding of various gene regulatory pathways in eukaryotes and eventually provided new approaches for drug discovery. RNAi has even been shown to be beneficial in silencing overexpressed genes in cancers. Thus, RNAi therapy

became mainstream was thought to have potential in the clinic for treating various diseases.

Unfortunately, there are limitations to RNAi therapy. Shortly after the concept for the therapy was proposed, researchers began to investigate its true potential. These initial studies resulted in disappointment and started changing people's view on the therapies potential. The siRNA had poor cellular internalization and the stability of siRNA in human plasma was abysmal. The overall negative surface charge of cell membranes repelled the negatively charged siRNA and highly restricted their ability to penetrate and enter the cells [156, 157]. The stability issues of siRNA resulted from the vast amount of nucleases present in human serum [158]. Later it was noticed that even if the siRNA was not degraded by nucleases, they had an extremely short half-life because their small size resulted in rapid excretion through the urine.

Luckily the concept of RNAi therapy was not completely lost on all researchers. While naked siRNA injected into biological systems resulted in disappointment, certain investigators studied ways to improve these limitations by utilizing DDSs. The siRNA can be complexed to a DDS, which can improve their cellular internalizations. At the same time, these complexes protect the siRNA from nucleases and increase their half-life within biological systems [158]. Protecting the siRNA using DDSs can improve cellular transfection and reestablishes the potential RNAi therapy was first thought to have in the clinic.

2.5 Drug Delivery Systems

Over the past few decades, interest in DDSs has continually increased. The pharmaceutical industry has incorporated various DDS formulations to their pipeline to improve the efficacy of novel therapeutic agents and their existing FDA-approved products. As mentioned earlier, the reason DDSs have become popular is the fact that they can improve on the existing pharmacokinetic (PK) and pharmacodynamics (PD) properties of a therapeutic entity [12-16, 159]. DDSs can be designed from many types of materials such as lipids, metals, and synthetic polymers. Popular approaches for utilizing DDSs include simple drug-polymer conjugation, drug entrapment matrices, and nanoparticle encapsulation of drugs [160]. The following study focuses on DDS formulations of liposomes and dendrimers.

2.5.1 Liposomes

Liposomes are spherical vesicles that consist of one or multiple concentric lipid bilayers enclosing an aqueous core (Figure 2.9) [161-163]. Liposomes can be produced from cholesterols, glycolipids, long-chain fatty acids, and sphingolipids; though they are primarily made using phospholipids today [164]. In the early 1960's, these vesicles were discovered when Bangham and his colleagues observed smears of egg lecithin would react with water to spontaneously form these intricate vesicles [165]. For years following their discovery, liposomes were

primarily utilized as artificial membranes to mimic simple cellular systems and investigate various properties such as permeation, transport mechanisms, and fusion kinetics [166, 167]. Nevertheless, it didn't take long for scientists to recognize their potential as DDSs. Early liposome formulations were developed to encapsulate therapeutic agents such as water-soluble small molecule drugs, nucleotides and proteins within their aqueous core [164, 168, 169]. Since then, liposome formulations have been developed to entrap hydrophobic drugs within their lipid bilayer and deliver them safely within cells [170-173].

Formulating liposomes with different types of lipids can alter their surface charge and other properties of the DDS. Zwitterionic lipids such phophatidylcholines and phophatidylethanolamines have the potential to different charges based on the environmental pH, but are neutral at physiological pH (7.4) and tend to produce neutral liposomes when prepared. Phosphatidylserines are phospholipids that carry a negative charge at physiological pH and generate negatively charged liposomes when prepared. Alternatively, lipids such as 1, 2-dioleoyl-3-trimethylammonium-propane (DOTAP) contain a positive charge at physiological pH and form cationic liposomes when prepared [174-176].

Since siRNA are macromolecules that hold an overall negative charge, they are able to form complexes with the surfaces of cationic liposomes. Liposome-mediated delivery is one method that has been utilized for cellular transfection of siRNA [177]. One limitation to using cationic liposomes is they can be cytotoxic if

their surface charge is too strong [178]. Therefore, formulating cationic liposomes with a combination of cationic, anionic, and even zwitterionic lipids can dampen the overall positive charge making the liposomes less toxic.

Liposomes have other limitations as DDSs as well. To start, liposomes tend to be rapidly cleared from circulation by the reticulendothelial system (RES) once detected by phagocytes [179]. Nevertheless, research has been conducted to overcome this limitation and researchers have discovered as rather simple method for reducing liposomal detection. If the surface of the liposomes is coated with polyethylene glycol (PEG), they develop a “stealth effect” and are able to escape recognition by phagocytes [180-183]. Another limitation for liposomes is that when they contained a charged surface (both anionic and cationic), is they tend to bind plasma proteins. Once they bind these proteins, they become recognized and are rapidly removed from circulation. To overcome this limitation, liposomes can be formulated with saturated phosphatidylcholines, which increase steric stabilization and reduce protein binding of the DDS [180, 184].

There are several mechanisms by which liposome-mediated cellular internalization works. One mechanism is that the liposomes attach to the cells and fuse with the cell membrane. As the phospholipids fuse with the membrane and incorporate themselves, pores begin to form in the vesicle. The contents begin to leak out of these pores and are released into the cytoplasm. This mechanism is a passive internalization and is characteristic of non-targeting

liposomes [164]. Another mechanism involves receptor-mediated endocytosis (Figure 2.10). Ligands conjugated to the liposome interact with their corresponding receptor and are internalized into the cell as an endosome forms around the DDS. The endosome migrates further into the cell and the contents are released when the liposome is digested by lysosomes. This is considered as active internalization and is characteristic of targeting liposomes that contain a targeting moiety for cell-specific internalization [185, 186].

2.5.2 Dendrimers

Polymer DDSs have been investigated immensely for their potential for improving the therapeutic efficacy of drugs for many years. These polymers can be covalently bound to drugs as well as entrapping them inside a matrix. Using polymers DDSs can improve water solubility, increase cellular permeability, increase drug stability, and decrease off-site cytotoxicity of drugs [187, 188]. Similar to liposomes, they can be conjugated to targeting moieties for cell-specific delivery of therapeutics. Dendrimers are a newer class of polymer-based DDS with a highly branched molecular structure. The term dendrimer stems from the Greek word Dendron. The literal translation of Dendron is tree, which makes sense since they are branched structures. Dendrimers are comprised of three distinguished components: an initiator core, interior layers (referred to as generations), and an exterior surface containing functional groups (Figure 2.11). Dendrimers can be synthesized using different molecules as the initiator core

and can contain multiple functional groups that can alter what purpose their serve [189-191].

Vögtle and colleagues first carried out controlled syntheses of dendrimers in 1978 [192]. However, dendrimers were not noticed for their potential as a DDS until the 1990's [193]. Dendrimers have defined structures and can be produced with high precision in an algorithmic fashion unlike other types of polymer-based DDSs that tend to have high polydispersity when prepared [187, 188, 194]. This means different batches can be produced with the same size, shape and functionality, making them an ideal DDS to develop novel therapeutic formulations.

Dendrimers can be synthesized by two well-defined techniques known as the divergent and convergent methods. Synthesis using the divergent method begins with at the initiator core and augments outward via serial Michael reactions [195]. The convergent method synthesizes dendrimers in the opposite direction as the divergent method. Small molecules that are used as surface functional groups once the particle is formed are subjected to serial reactions that build inward and are eventually bound to the core molecule [196]. Out of the two synthesis methods, divergent dendrimer synthesis has become more popular today. It reactions tend to be more successful and is commonly used for large scale synthesis of dendrimers such as Poly(amido amino) PAMAM, Poly(propylenimine) (PPI), Tecto, and micellar dendrimers [197].

Van Den Berg and Meijer developed PPI dendrimers, also known as Astramol dendrimers, in 1993 [198]. PPI dendrimers contain a butylenediamine molecule as the initiator core. They contain a cationic surface due to the amine functional groups that line the surface of the structure (Figure 2.12). The cationic surface allows them to bind nucleotides, making them an excellent DDS for nucleotide delivery [199, 200]. Schatzlein and colleagues investigated quaternized PPI dendrimers and showed they could be used as a gene therapy vector in an animal model [201]. Chen and colleagues demonstrated that generation 4 PPI dendrimers enhanced the cellular internalization of oligodeoxynucleotides in MDA-MB-231 breast cancer cells [199]. For this study, we investigated the capability of PPI dendrimers to enhance the cellular internalization of siRNA in ovarian cancer cells.

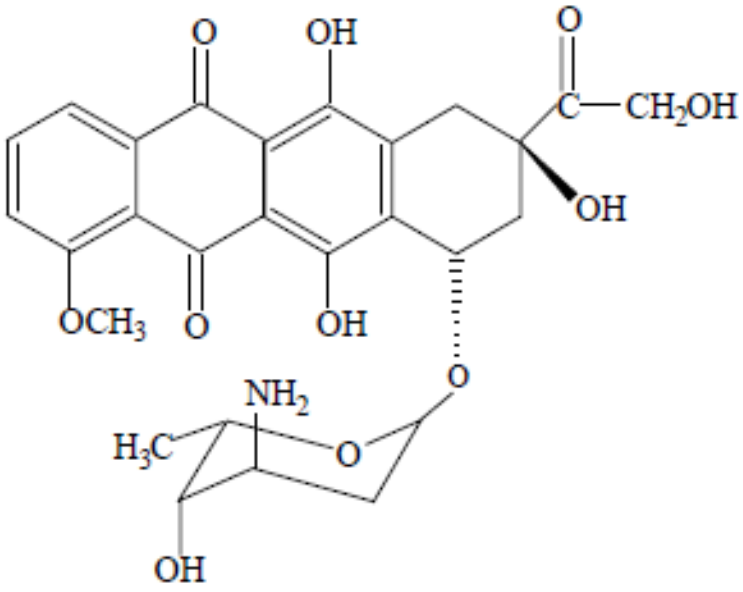

Figure 2.1: The chemical structure of Doxorubicin (Reproduced from Ref. [48])

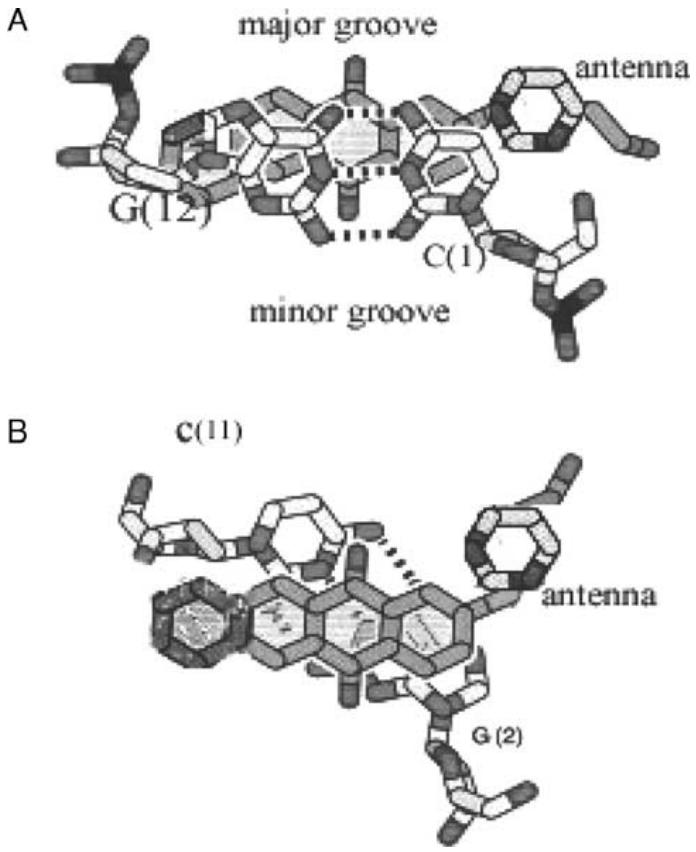

Figure 1.2: Axial views of intercalated DNA for dox: (A) the C (1)–G (12) base pair over dox: (B) the C (11)–G (2) base pair over dox. (Reproduced from Ref. [48])

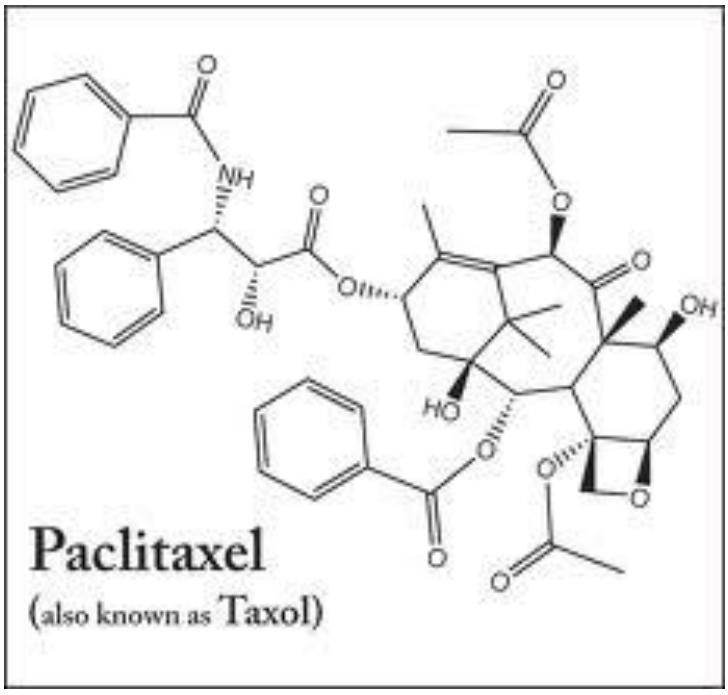

Figure 1.3: The chemical structure of Paclitaxel (Reproduced from Ref [73])

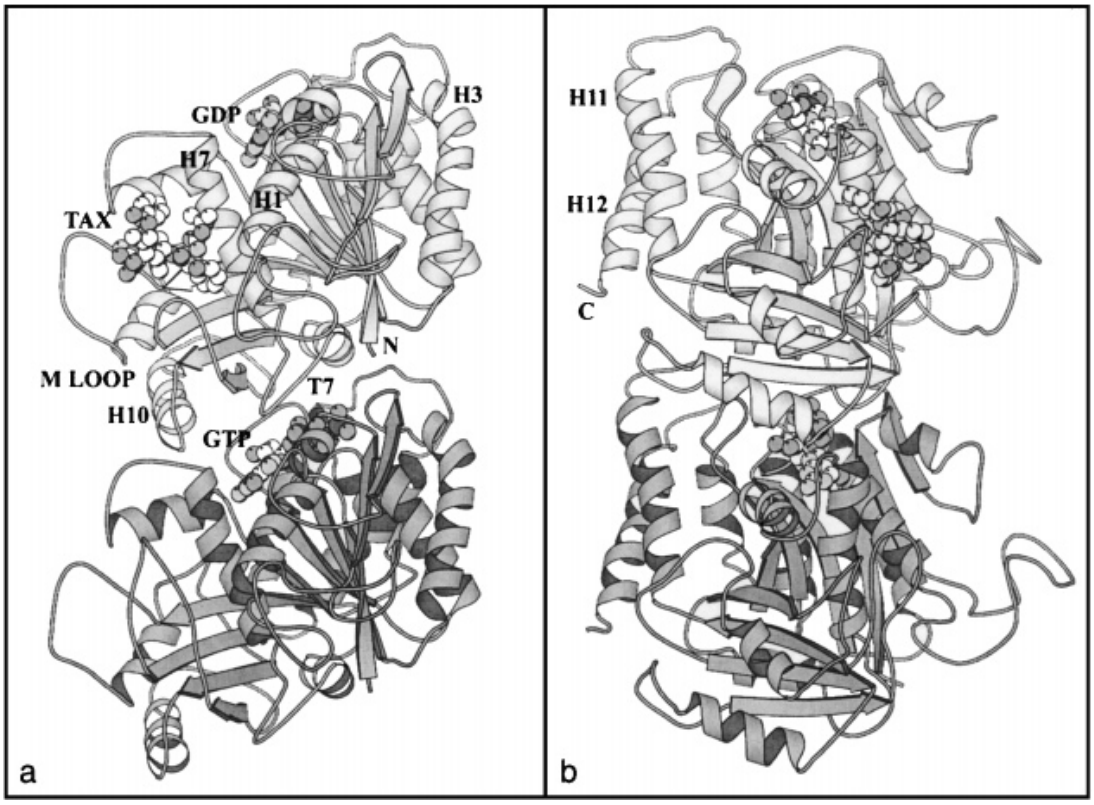

Figure 2.4: Ribbon diagram of the tubulin dimer (a) as seen from the inside of the microtubule and (b) seen from the left side of (a). The β monomer is at the top, which would correspond to the plus end of a microtubule. Atomic structures are shown for the nucleotides (GTP and GDP) and a molecule of taxotere (TAX). Several of the secondary structure elements referred to in the text are indicated. Note that the sequence numbering scheme used here is based on alignment of α and β sequences. (Reproduced from Ref. [63])

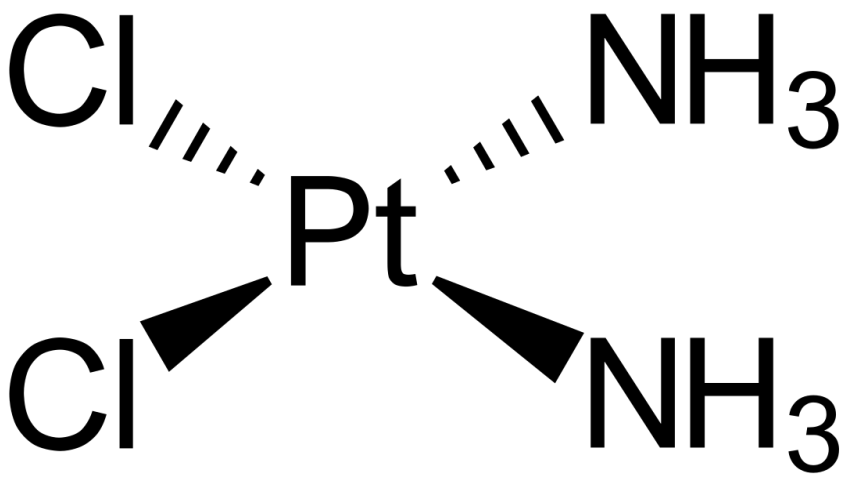

Figure 2.5: The chemical structure of Cisplatin (Reproduced from Ref. [84])

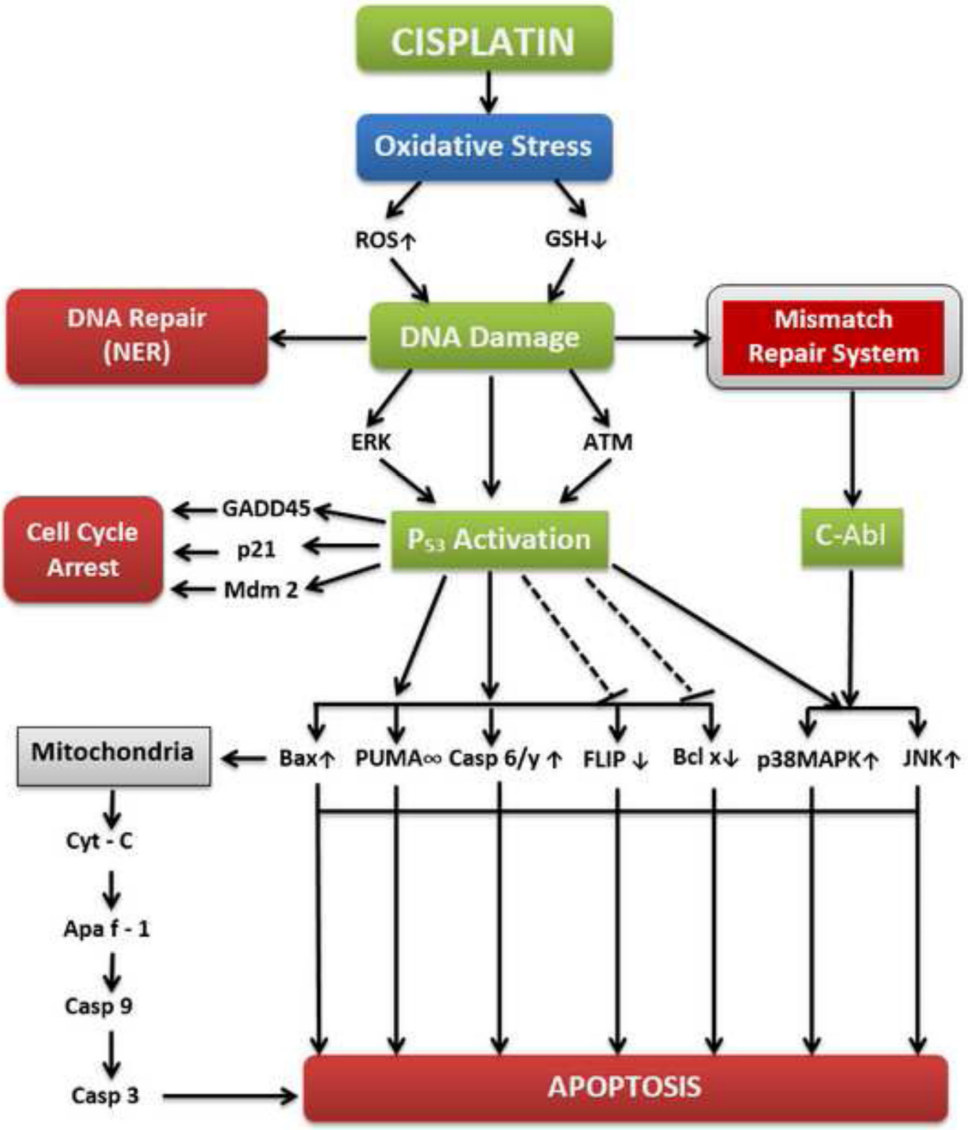

Figure 2.6: Overview of molecular mechanisms of cisplatin in cancer treatment. (Reproduced from Ref. [84])

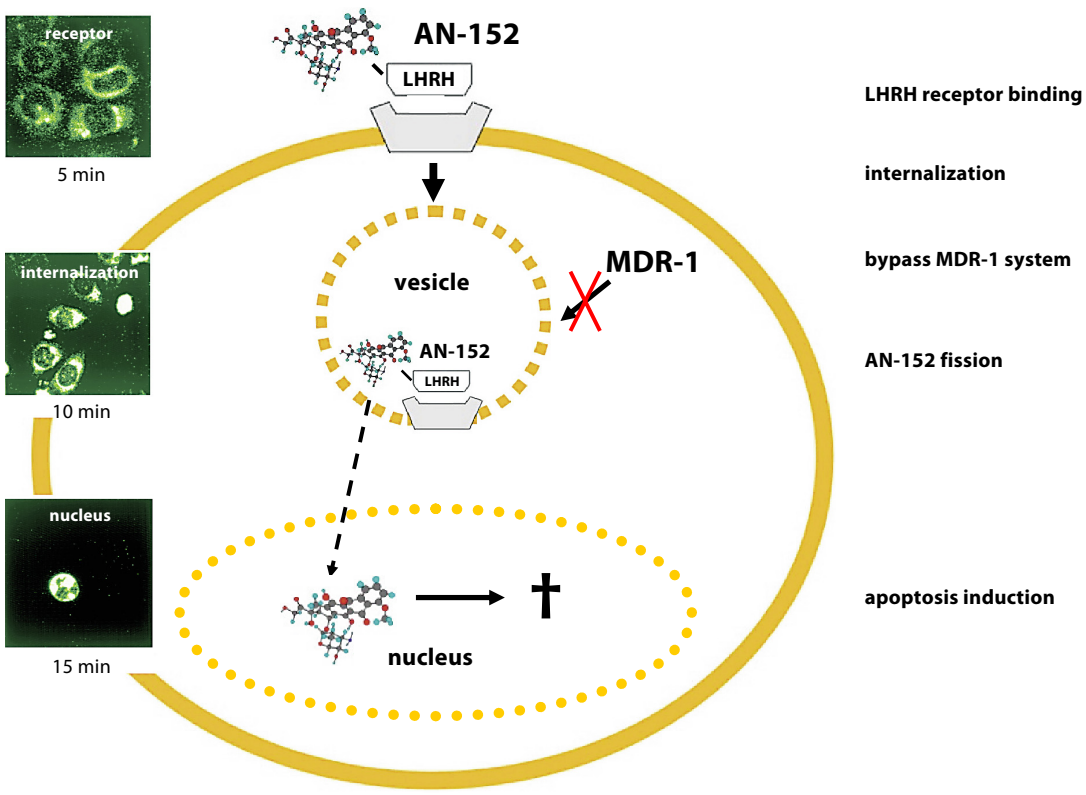

Figure 2.7: Internalization of the cytotoxic LHRH analogue AN-152 induces multidrug resistance gene (MDR-1)-independent apopto- sis. After receptor binding, the AN-152/LHRH receptor complex is internalized via coated vesicles bypassing the multidrug resis- tance-1 system. (Reproduced from Ref. [140])

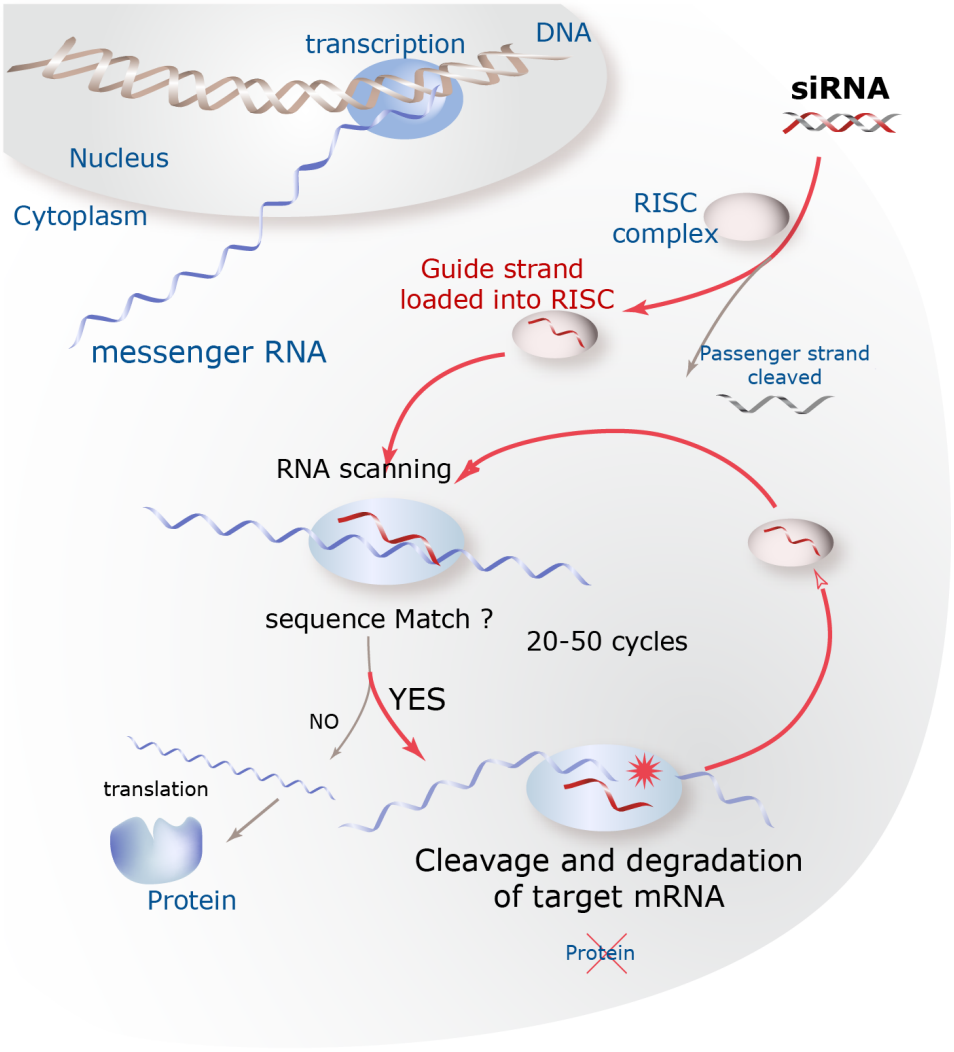

Figure 2.8: Mechanism in which RNA interference is achieved. (Reproduced from Ref. [202])

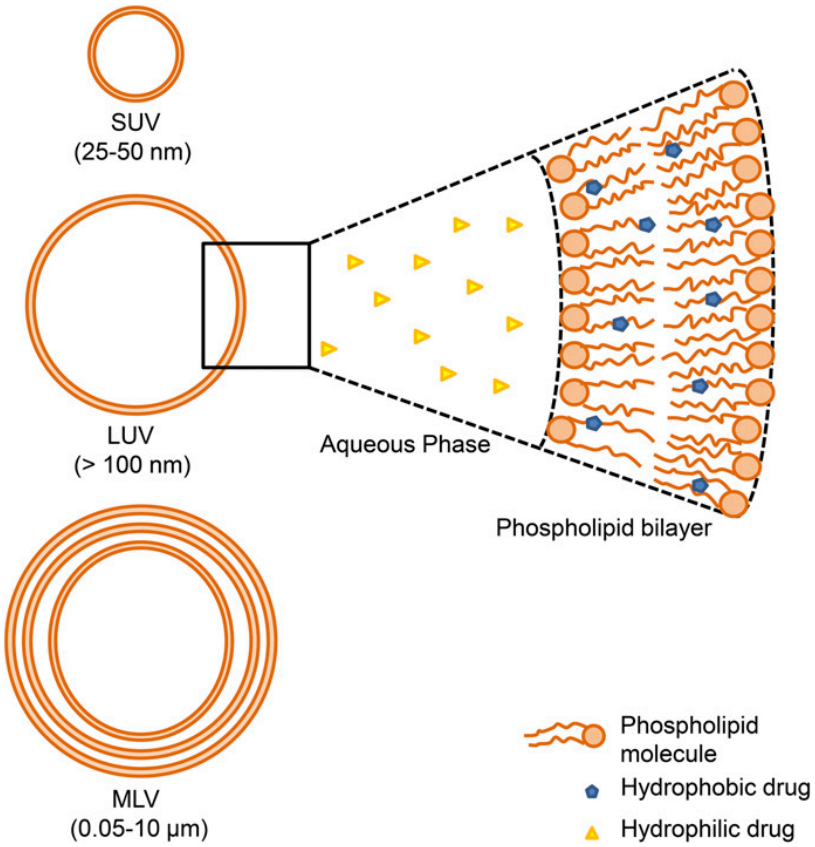

Figure 2.9: Types of liposomes classified by size and lamellarity. Based on size and lamellarity, liposomes can be classified into 3 different types: multilamellar vesicles (MLVs), large unilamellar vesicles (LUVs), and small unilamellar vesicles (SUVs) are usually in the size range of 25–50 nm and, like LUVs, consist of a single phospholipid bilayer. (Reproduced from Ref. [185])

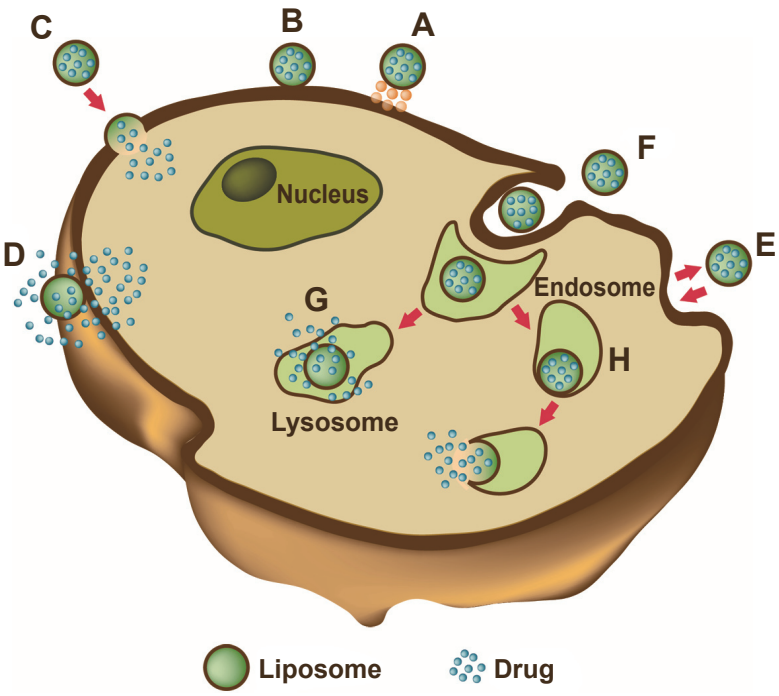

Figure 2.10: Liposomes binding to the surface through receptors (A). Absorption onto the plasma by electrostatic interactions (B). The delivery of the cargo into the cell cytoplasm can take place through different modes. Lipid nanocarriers fuse with the plasma membrane and discharge drugs into the cell (C). The structure of the liposome bilayer can be affected and the cargo is released (D). exchange of carrier-lipid components with the cell membrane can also occur (E). Internalized by endocytosis (F) can have different fates depending on physicochemical characteristics. endosomes fuse with lysosomes (G): in this case, the low pH induces the degradation of the liposome membrane and the drug is released. endosomes follow another route (H): liposomes release their cargo after fusion or the destabilization of the endocytic vesicle. (Reproduced from Ref [186])

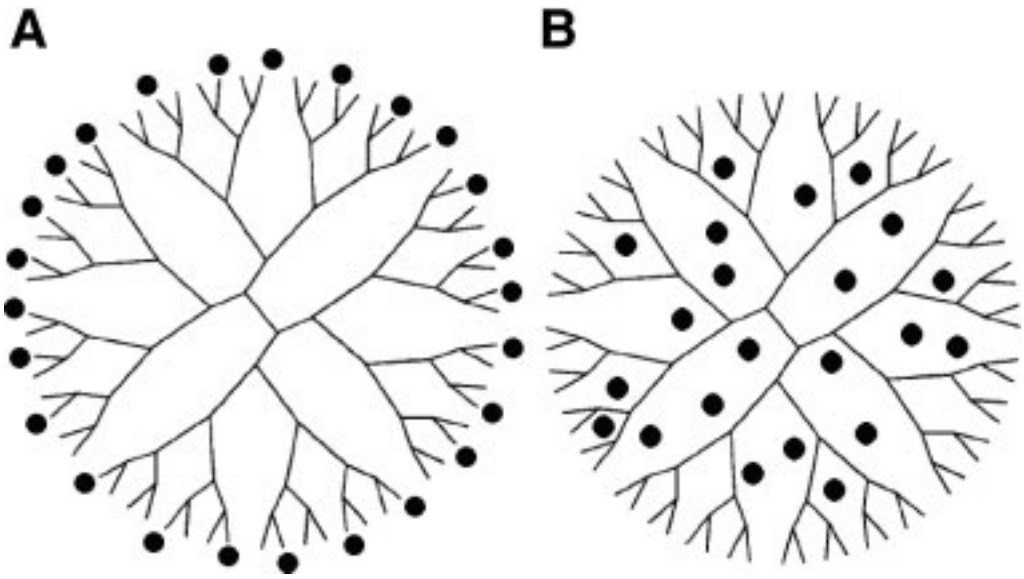

Figure 2.11: Potential strategies for interactions bet- ween dendrimers and drug molecules (A) electrostatic interactions or covalent conjugate, and (B) simple encapsulation. (Reproduced from Ref. [190])

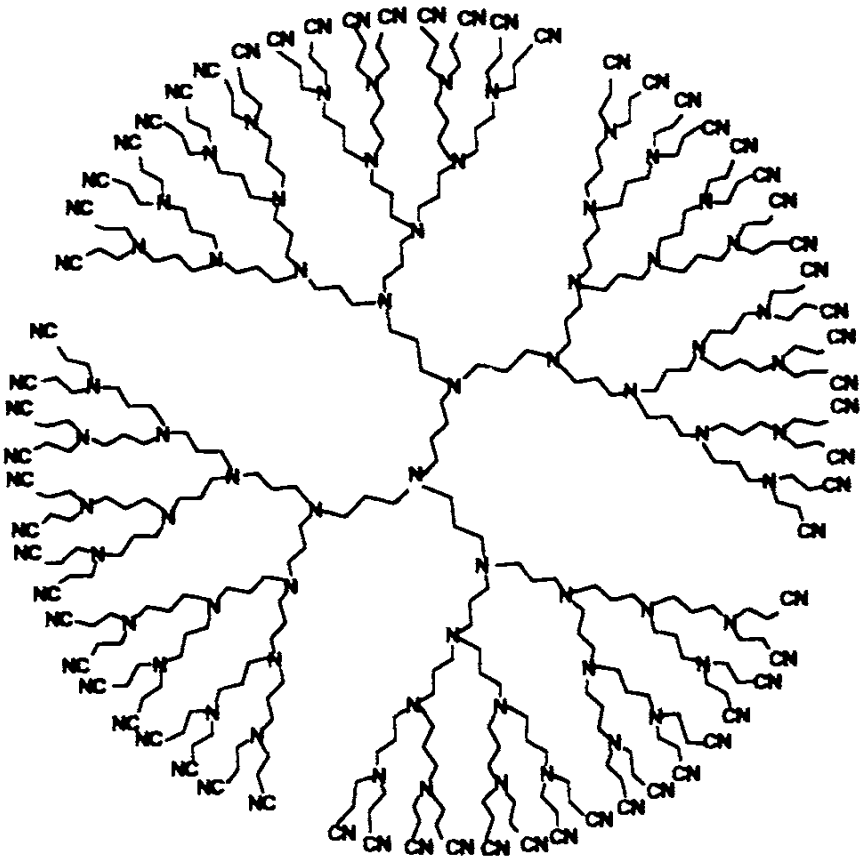

Figure 2.12: Synthetic scheme for poly(propy1ene imine) dendrirners with di-aminobutane as core. (Reproduced from Ref. [198])

3 SPECIFIC AIMS

Specific Aim 1: Deriving Primary Tumor Isolates for Use in Precision Cancer Therapy and Evaluation of Patient Gene Expression Profiles

Over the decades, one characteristic of cancer that all researchers emphasize is the extreme complexity it can have in different patients [92-94]. This shaped the way oncologists view different types of cancers originating in different organs. Additionally, it has become increasing evident that there are significant mechanisms leading to cancer progression among patients with the same type of cancer and this has led to patients being further stratified into different subtypes of the disease [95-98]. Also, traditional chemotherapeutic agents fail to differentiate between the cancerous cells and normal healthy cells. Since these agents are designed to eliminate tumors by causing cell death, they will kill any cell they interact with inside the body [8]. This indiscriminate destruction can cause damage to healthy non-target tissues and organs, leading to adverse side effects and toxicity issues in patients receiving the treatment. As a result, precision cancer medicine is now a major focus to researchers.

In order to develop optimal treatment regimens for individual cancer patients, oncologists need to learn more about the molecular biology of the patient. More importantly molecular analysis of patient biopsies are required to better understand a patient’s cancer and predict prognoses of available treatments.

One technique that is becoming more mainstream as research advances is transcriptome profiling.

Transcriptome profiling to identify gene expression patterns in cancer patients can be very useful for developing precision therapies. Genetic dysregulation is the basis for cancer development and progression [107-109]. Analyzing transcriptome profiles can help oncologists better understand the underlying mechanisms causing the disease in patient populations and even in individuals. This could further stratify patients on a molecular level for more detailed disease subtypes. One method for obtaining patient transcriptome profiles is quantitative reverse transcription polymerase chain reaction (qRT-PCR). This technique can allow oncologists to visualize gene expression dysregulation within cancerous cells in a short period of time and in a relatively cost effective manner. Due to technological advancements, the costs of running this experiment are becoming cheaper. Also as the field of automatized engineering further develops, more products are becoming commercially available to make this process fully automated [203, 204]. Not only will that allow the technique to be run faster, but it also will reduce the amount of human error involved in the procedures making it more efficient.

Once a patient's transcriptome has been profiled, it can aid oncologists in many ways. Subtype-specific gene signatures have been shown to help predict treatment response, tumor progression, and even patient prognosis [121-124]. It

can also be used for targeting certain genes using RNAi therapy. RNAi therapy can be used to target overexpressed genes in a patient's tumor. The genes could be involved in disease progression and drug resistance mechanisms. By targeting a set of overexpressed genes, their role in the disease can be diminished through the gene silencing resulting from the therapy. This could allow certain chemotherapeutic agents to become for efficacious in patients that typically would have no response from the treatment. However, it is known that not all genes in the human genome are equally capable for cancer development. Therefore, it is not necessary to profile a patient's entire transcriptome. This would not be cost effective and an efficient way for developing RNAi therapies.

In this current study, we propose a precision combinational therapy (co-therapy) that utilizes transcriptome profiling and RNAi therapy in order to raise the efficacy of small molecule chemotherapeutics that are currently FDA-approved for treating patients with ovarian cancer. Numerous patient biopsies will be analyzed to develop an optimal array of genes extremely pertinent in ovarian cancer development and progression. To do this, our team collaborated with the Robert Wood Johnson Medicinal School to obtain patient biopsies. These patient biopsy samples will be utilized to create primary tumor isolate cultures and subjected to qRT-PCR to analyze a total of 191 genes known to be involved in apoptosis regulation, breast cancer, and ovarian cancer. From these list of genes, we narrowed the number of genes to 84 in order to make the analysis process more streamlined.

Specific Aim 2: Categorization and Optimization of Nanoparticle-Based Formulations for Delivering of Chemotherapeutic Drugs and Nucleic Acids

The prosed co-therapy in this study utilized RNAi therapy and small molecule chemotherapy. For the RNAi therapy, siRNA macromolecules were used as the therapeutic agents. When naked siRNA is injected into systemic circulation, it has a number of problems that make it challenging to be effective in treating patients. First, siRNA has poor stability in the blood plasma. This is due to proteases that quickly degrade the molecules when they come into contact [158]. This mean most of them will be broken down way before they reach the desired site of action. Another issue with treating patients with naked siRNA is they have an extremely short half-life in the body due to their small molecular size. The siRNA molecules are quickly filtered into the urine by the kidneys. This quick elimination combined with their instability in blood plasma has been shown to give siRNA a half-life of roughly one minute inside the body. Not only that, there is one other property of nucleotide that give them no chance of being effective as therapeutic agents when naked siRNA is introduced to the body. All nucleotide have an anionic charge. The overall surface charge of cell membranes is also anionic. Consequently, naked siRNA cannot penetrate the cell membrane due electrostatic repulsion [156, 157]. Resulting in none of the siRNA internalizing into the cells to downregulate the expression of the target gene(s). All of these challenges can be overcome by using nanoparticle DDSs. They can complex the

siRNA, protect it from degradation, and help facilitate cellular internalization of these nucleotides [158].

Traditional chemotherapeutic agents fail to differentiate between the cancerous cells and normal healthy cells. Since these agents are designed to eliminate tumors by causing cell death, they will kill any cell they interact with inside the body. This indiscriminate destruction can cause damage to healthy non-target tissues and organs, leading to adverse side effects and toxicity issues in patients receiving the treatment [8]. The pharmaceutical industry has incorporated various DDS formulations to their pipeline to improve the efficacy of novel therapeutic agents and their existing FDA-approved products. As mentioned earlier, the reason DDSs have become popular is the fact that they can improve on the existing pharmacokinetic (PK) and pharmacodynamics (PD) properties of a therapeutic entity [12-16, 159]. Targeted delivery of conventional chemotherapeutics, specifically to cancer cells, can reduce off-target disposition of the chemotherapeutics and the adverse side effects that accompany this disposition. By exploiting overexpressed cell surface receptors, it is possible to increase the accumulation of chemotherapeutics at the desired site of action. Ligands that interact with the overexpressed receptors can be conjugated to a drug and have been shown to increase its delivery and internalization of specific cells [9, 128-132].

In the current study, we investigated two different types of nanoparticle DDSs; liposomes and dendrimers. We categorized multiple formulations of both DDSs and investigate which would be optimal for our proposed co-therapy. The work below describes and illustrates the properties of each formulation and which ones were chosen for further experimentation.

Specific Aim 3: Evaluation of the Therapeutic Efficiency of the Various Targeted Nanotechnology-Based Chemo/siRNA Combinatorial Delivery Systems

The current 5-year survival rate for patients with advanced-stage ovarian cancer is a meager 30% [5-7]. This can be accredited to the fact that the disease has become highly invasive and multidrug resistant by the time it has been diagnosed in most patients. Most treatments can help reduce and possible eliminate the primary tumor, but a lot of patients have metastatic recurrent tumors that develop after treatment ends [205, 206].

As a result, targeted therapeutics has become one of the main focuses in oncology research to improve the issues with toxicity in patients. Targeted therapeutics exploit abnormalities resulting from disease progression and are not present in healthy cells, tissues and organs [9-11]. As mentioned earlier, nanoparticle drug delivery systems (DDSs) have demonstrated great potential for precision treatment of cancer. By conjugating a certain ligand to a DDS,

specifically one that can interact with a cell surface receptor expressed in the diseased states, it acquires the ability to target those cells and produces higher concentrations at the target site of action [20-24].

Here, we investigated the therapeutic efficacy of our proposed co-therapy system using multiple drugs. We already analyzed patient gene expression profiles and optimized our nanoparticle DDSs. We evaluated the co-therapy using our liposomal DDS *in vitro* and are current developing an animal model for evaluating its efficacy *in vivo*. Based on previous work in our lab [141, 156, 207, 208], we knew the potential for our dendrimer DDS *in vtiro* and proceeded to investigate it's efficacy in animal models for *in vivo* evaluation.

4 Deriving Primary Tumor Isolates for Use in Precision Cancer Therapy and Evaluation of Patient Gene Expression Profiles

4.1 Introduction

It has become imperative that researchers stress the extreme complexity and high variability cancers can have in different patients [92-94]. Not only has this shaped oncologists view different types of cancers originating in different organs, but also between patients of the same type of cancer and this has led to patients being stratified into different subtypes of the disease [95-98]. Also, Traditional chemotherapeutic agents fail to differentiate between the cancerous cells and normal healthy cells. Since these agents are designed to eliminate tumors by causing cell death, they will kill any cell they interact with inside the body [8]. This indiscriminate destruction can cause damage to healthy non-target tissues and organs, leading to adverse side effects and toxicity issues in patients receiving the treatment. As a result, precision cancer medicine is now a major focus to researchers.

In order to develop optimal treatment regimens for individual cancer patients, oncologists need to learn more about the molecular biology of the patient. More importantly molecular analysis of patient biopsies are required to better comprehend a patient's cancer and predict prognoses of available treatments. One technique that is becoming more mainstream as research advances is transcriptome profiling.

Transcriptome profiling to identify gene expression patterns in cancer patients can be very useful for developing precision therapies. Genetic dysregulation is the basis for cancer development and progression [107-109]. Analyzing transcriptome profiles can help oncologists better understand the underlying mechanisms causing the disease in patient populations and even in individuals. This could further stratify patients on a molecular level for more detailed disease subtypes.

One method for obtaining patient transcriptome profiles is quantitative reverse transcription polymerase chain reaction (qRT-PCR). This technique can allow oncologists to visualize gene expression dysregulation within cancerous cells in a short period of time and in a relatively cost effective manner. Due to technological advancements, the costs of running this experiment are becoming cheaper. Also as the field of automatized engineering further develops, more products are becoming commercially available to make this process fully automated [203, 204]. Not only will that allow the technique to be run faster, but it also will reduce the amount of human error involved in the procedures making it more efficient.

Once a patient's transcriptome has been profiled, it can aid oncologists in many ways. Subtype-specific gene signatures have been shown to help predict

treatment response, tumor progression, and even patient prognosis [121-124]. It can also be used for targeting certain genes using RNAi therapy.

RNAi therapy can be used to target overexpressed genes in a patient's tumor. The genes could be involved in disease progression and drug resistance mechanisms. By targeting a set of overexpressed genes, their role in the disease can be diminished through the gene silencing resulting from the therapy. This could allow certain chemotherapeutic agents to become for efficacious in patients that typically would have no response from the treatment. However, it is known that not all genes in the human genome are equally capable for cancer development. Therefore, it is not necessary to profile a patient's entire transcriptome. This would not be cost effective and an efficient way for developing RNAi therapies.

In this current study, we propose a precision combinational therapy (co-therapy) that utilizes transcriptome profiling and RNAi therapy in order to raise the efficacy of small molecule chemotherapeutics that are currently FDA-approved for treating patients with ovarian cancer (Figure 4.1). Numerous patient biopsies will be analyzed to develop an optimal array of genes extremely pertinent in ovarian cancer development and progression. To do this, our team collaborated with the Robert Wood Johnson Medicinal School to obtain patient biopsies. These patient biopsy samples will be utilized to create primary tumor isolate cultures and subjected to qRT-PCR to analyze a total of 191 genes known to be involved in

apoptosis regulation, breast cancer, and ovarian cancer. From these list of genes, we narrowed the number of genes to 84 in order to make the analysis process more streamlined.

4.2 Material and Methods

4.2.1 Materials

Ovarian cancer patient biopsies were obtained from volunteers involved in research studies at the Cancer Institute of NJ affiliated with Robert Wood Medicinal School within Rutgers University (Piscataway, NJ, USA). Healthy ovarian tissues were purchased from ATCC (Manassas, VA, USA). Cellstar® sterile cell culture flasks (25 cm2 and 75 cm2) and centrifuge tubes (15 mL and 50 mL) were purchased from Greiner Bio-One GmbH (Monroe, NC, USA). BioWhittaker® Dulbecco's Phosphate Buffered Saline (DPBS) and RPMI-1640 with L-Glutamine culture media were purchased from Lonza Group AG (Morristown, NJ, USA). USA-sourced Fetal Bovine Serum (FBS) for mammalian cell cultures and 2-Mercaptoethanol (BME) were purchased from Sigma-Aldrich Inc. (St. Louis, MO, USA). Gibco brand Penicillin-Streptomycin culture supplement (Pen-Strep), sodium bicarbonate (7.5%), and trypsin-EDTA (0.05%) solutions were purchased from ThermoFisher Scientific Inc. (Waltham, MA, USA). QIAshredder®, RNeasy® Mini kit, RT2 First Strand Kit, RT2 SYBR® Green ROXTM qPCR Mastermix, RT2 ProfilerTM PCR Array (Human Apoptosis

and Human Breast Cancer), and qBiomarker Copy Number PCR Array, Human Ovarian Cancer products were all purchased from Qiagen (Hilden, Germany). GeneMate DNase/RNase free microtubes and SnapStrip II tubes were purchased from BioExpress (Radnor, PA, USA).

4.2.2 Deriving Primary Tumor Isolates

Patient biopsies obtained from the Cancer Institute of New Jersey were cryopersevered immediately after removal from patients and shipped to our lab. RMPI-160 media was prepared with 10% FBS, 5% sodium bicarbonate, and 2.5% Pen-Strep once the samples arrived. Primary tumor isolate cultures were derived using the explant tissue culture method as follows. Biopsies samples were thawed slowly, sterilized using ethanol washes and Pen-Strep washes. After sterilization, cuts were made into the sample and each piece was placed into a cell culture flask containing the prepared RPMI-1640 media. The media was changed every day and the samples were observed under a microscope for signs of primary cell outgrowth. The cellular outgrowth eventually formed a “halo” around the biopsy sample. AT this point, the sample was transferred to a new flask and the cells in the original flask were cultured further. After a few days, the cells were trypsinized and transferred to a new flask. This process was repeated until flasks became confluent. The cells were then collected and cryopreserved in liquid nitrogen until enough samples formed primary tumor isolates cultures and further experimentation in the study could proceed.

4.2.3 RNA Extraction and Purification

Once the primary tumor isolate cultures were grown to confluence, the media was removed, the cells were washed twice using DPBS, and incubated with trypsin-EDTA (0.05%) for 5 minutes. Media was added to the culture flasks to end trypsinization and help remove any cells still slightly attached. The cells were then collected in conical centrifuge tubes, spun down to form a cell pellet, and the supernatant was aspirated.

Total RNA extraction and purification was performed using the RNeasy Mini Kit as follows. Cell lysis was performed by adding RLT buffer (containing added BME) to the centrifuge tube containing the cell pellet and mixed by pipetting until the cell pellet was no longer visible. The lysate was then homogenized using a QIAshredder spin column and centrifuged at 13.2x103 RPM. 70% ethanol was added to the sample supernatant and was transferred to an RNeasy spin column. Once in the spin column, the sample was centrifuged at 1x104 RPM for 15 seconds and the flow-through was discarded. RW1 buffer was added to the spin column and centrifuge at 1x104 RPM for 15 seconds and the flow-through was discarded. Next, RPE buffer (containing added ethanol) was added to the spin column and centrifuged at 1x104 RPM for 15 seconds and the flow-through was discarded. Additional RPE buffer (containing added ethanol) was added to the spin column and was centrifuged at 1x104 RPM, but this time centrifugation was

set for two minutes. At this point, the RNA was considered purified. To collect the purified RNA, RNase-free water was added to the spin column and centrifuge at 1x104 RPM for one minute to elute the RNA. The collected RNA was measured using a Nanoquant Infinite m200 (Tecan Trading AG, Switzerland) to quantify the concentration and purity of each sample.

4.2.4 Reverse Transcription

Reverse Transcription (RT) was preformed to synthesize cDNA for each sample using the RT2 First Strand Kit as follows. First, a genomic DNA elimination mix was prepared containing 1,200 ng total RNA, genomic elimination (GE) buffer, and RNase-free water. This was done to ensure any residual genomic DNA still present in the sample after RNA extraction was removed so it would not produce faulty gene expression data in our experiments. Each component of the mix was added to a sterile tube, mixed gently by pipetting, and centrifuged briefly to ensure all of the mix was at the bottom of the tube. Once prepared, the genomic DNA elimination mix was incubated for five minutes at 42 0C and immediately placed on ice for at least one minute following incubation. During incubation, a RT mix was prepared containing a pH buffer (BC3), reverse transcriptase premix (RE3), and RNase-free water. After the genomic DNA elimination mix was left on ice for long enough and chilled, the RT mix was added to it in a 1:1 volume ratio and mixed gently by pipetting. The combined mix was then incubated for 15 minutes at 42 0C to allow RT to occur in the sample. Once this period was

complete, the mix was incubated for five minutes at 95 0C to denature the reverse transcriptase and stop the reaction. RNase-free water was added to the tubes to dilute the samples. The samples were either used immediately for quantitative real-time polymerase chain reaction (qRT-PCR) or stored at -20 0C to be used for the reaction at a later date.

4.2.5 Quantitative Real-Time Polymerase Chain Reaction

The expression levels of 191 different genes were quantified for each sample by quantitative real-time polymerase chain reaction (qRT-PCR) using three predesigned RT2 Profiler PCR Arrays (96-well format). The arrays contained genes known to be associated with apoptosis, breast cancer, and ovarian cancer (Figure 4.1). Each sample was prepared for qRT-PCR as follows. A PCR components mix was prepared with synthesized sample cDNA, RT2 SYBR Green mastermix, and RNase-free water. To ensure there was enough of this mix for all 96 wells in each assay, an extra 10% volume was prepared than required for 96 PCR reactions. Aliquots of the mix were transferred to each well of the plate, which contain lyophilized primers added by the manufacturer. Once the sample was aliquoted into all of the wells, an optical adhesive film was placed on the top of the plate to prevent loss of moisture at high cycle temperatures, and the plate was centrifuged in a 96-well plate centrifuge to remove any bubbles that may have formed during pipetting. Afterwards, the plate was placed into a StepOnePlus Real-Time PCR system (Applied Biosystems, Foster City, CA,

USA) to carry out the PCR reactions. The PCR system carried out the following cycling conditions. One cycle set for 10 min at 95 ^{0}C to activate the DNA Taq polymerase. Then the system conducted 40 cycles set for 15 seconds at 95 0C then one minute at 60 ^{0}C to perform the PCR and fluorescence data collection.

4.2.6 Generating Gene Expression Profiles

The StepOne software corresponding with the StepOnePlus Real-Time PCR system compiled data collected during qRT-PCR reactions. The software would calculate the threshold cycle (CT) for each reaction and these values were used to obtain the fold-change in expression for each gene investigated in the study. The software files containing the qRT-PCR results for every sample were exported as Microsoft Excel files and manually calculated as following. The results for the control sample (healthy ovarian tissue) were analyzed first followed by the experimental samples (primary tumor isolates) using the ΔΔCT method. First, the difference between the CT values (ΔCT) for each gene of interest (GOI) and the average CT value of the set of housekeeping genes (HKG) incorporated in each assay ($CT_{[GOI]}$ - $CT_{[HKGs\ average]}$). This calculation normalized the CT values of each GOI. Normalization was done on both the control and experimental samples. Next, the difference in ΔCT (ΔΔCT) between the two samples was calculated to determine the change in gene expression for each GOI ($\Delta CT_{[experimental]}$ - $\Delta CT_{[control]}$). Finally, the fold change in expression for each GOI was calculated. Fold change in expression is equal to $2^{(-\Delta\Delta CT)}$.

4.2.7 Statistical Analysis

Statistical analysis was performed on the obtained data using single factor analysis of variants (ANOVA) and presented the results as the mean value ± standard deviation from three independent measurements. Data sets were analyzed for significance using t-tests considered P values less than 0.05 to be statistically significant.

4.3 Results

4.3.1 Primary Tumor Isolates

Most biopsy samples were able to form primary tumor isolate cultures. Some of the samples did not grow well in the media, never formed viable primary tumor isolates, and were discarded. Other samples formed primary tumor isolates, but did not grow well after they were thawed from cryopreservation for further culturing. A total of 12 cultures remained the ability to be further cultured and were used in further to generate gene expression profiles.

4.3.2 Evaluation of Patient Gene Expression Profiles

A total of 7 patient samples were used to analyze gene expression levels. From the 191 genes analyzed, only 83 genes showed dysregulation in their expression levels compared to the healthy ovarian tissue (Figure 4.2). The genes we deemed significant were involved in various functions of cellular growth and regulation (Figure 4.3). The gene function groups include: angiogenesis, apoptosis regulation, cell cycle regulation, DNA damage repair, drug resistance, metalloproteases, signal transduction, and transcription factors.

4.4. Discussion

When we first received biopsy samples from the Cancer Institute of New Jersey, we had a total of 20 samples to use in our study. Unfortunately, not all of these samples were successful in becoming primary tumor isolates. From the 20, only 12 of them formed monolayers in culture and from these 12 sample cultures only 7 samples grew efficiently to obtain usable RNA concentrations when extracted and purified. Deriving primary tumor isolates can be a difficult and frustrating task as we learned from these samples. The 7 samples we did successfully extract adequate RNA levels from showed similar and slightly varying gene expression profiles (Figure 4.2). We selected our 83 genes because they showed the highest levels of expression dysregulation compared with healthy ovarian tissue and were deemed pertinent to ovarian cancer based on literature searches.

The reason we selected 83 genes for further patient screening is because the instrument we had for conducting qRT-PCR held 96 well plates. Therefore, we selected 83 genes we could use as possible targets in our RNAi therapy. The remaining spaces on the plate were used for housekeeping gene references and positive/negative reaction controls. One well was used to screen expression of LHRHR. Since this receptor will be exploited by conjugating LHRH to our DDSs, we wanted to make sure the individual patients expressed the cell-surface receptor to ensure the targeting moiety would be successful in targeting the cancerous cells. All of this fit onto one 96-well plate, which allowed us to more effectively, screen future patient samples obtained in the future.

4.5 Conclusions

Overall, we noticed some setbacks when deriving primary tumor isolates from all of our biopsy samples. Thankfully we were able to derive a good amount to them to continue the study. These primary tumor isolates allowed us to create a customized 96-well gene expression assay for future patients that could be included in further studies after this one.

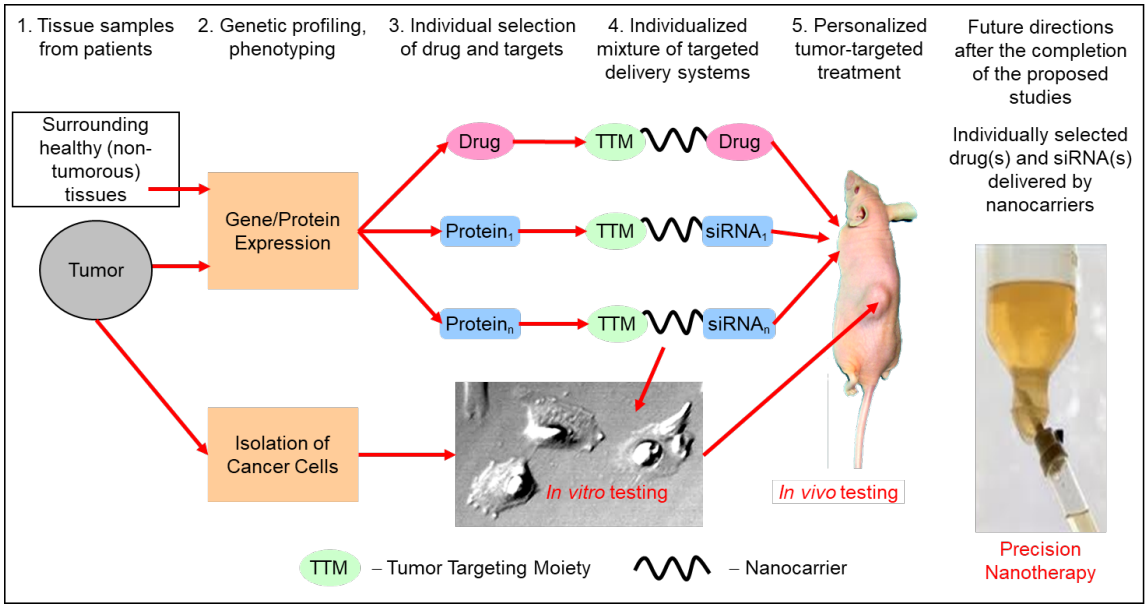

Figure 4.1: Overview of developing our proposed precision co-therapy. (Reproduced from Ref. [209])

A

	1	2	3	4	5	6	7	8	9	10	11	12
A	ABL1	AIFM1	AKT1	APAF1	BAD	BAG1	BAG3	BAK1	BAX	BCL10	BCL2	BCL2A1
B	BCL2L1	BCL2L10	BCL2L11	BCL2L2	BFAR	BID	BIK	BIRC2	BIRC3	BIRC5	BIRC6	BNIP2
C	BNIP3	BNIP3L	BRAF	CASP1	CASP10	CASP14	CASP2	CASP3	CASP4	CASP5	CASP6	CASP7
D	CASP8	CASP9	CD27	CD40	CD40LG	CD70	CFLAR	CIDEA	CIDEB	CRADD	CYCS	DAPK1
E	DFFA	DIABLO	FADD	FAS	FASLG	GADD45A	HRK	IGF1R	IL10	LTA	LTBR	MCL1
F	NAIP	NFKB1	NOD1	NOL3	PYCARD	RIPK2	TNF	TNFRSF10A	TNFRSF10B	TNFRSF11B	TNFRSF1A	TNFRSF1B
G	TNFRSF21	TNFRSF25	TNFRSF9	TNFSF10	TNFSF8	TP53	TP53BP2	TP73	TRADD	TRAF2	TRAF3	XIAP

B

	1	2	3	4	5	6	7	8	9	10	11	12
A	ABCB1	ABCG2	ADAM23	AKT1	APC	AR	ATM	BAD	BCL2	BIRC5	BRCA1	BRCA2
B	CCNA1	CCND1	CCND2	CCNE1	CDH1	CDH13	CDK2	CDKN1A	CDKN1C	CDKN2A	CSF1	CST6
C	CTNNB1	CTSD	EGF	EGFR	ERBB2	ESR1	ESR2	FOXA1	GATA3	GLI1	GRB7	GSTP1
D	HIC1	ID1	IGF1	IGF1R	IGFBP3	IL6	JUN	KRT18	KRT19	KRT5	KRT8	MAPK1
E	MAPK3	MAPK8	MGMT	MKI67	MLH1	MMP2	MMP9	MUC1	MYC	NME1	NOTCH1	NR3C1
F	PGR	PLAU	PRDM2	PTEN	PTGS2	PYCARD	RARB	RASSF1	RB1	SERPINE1	SFN	SFRP1
G	SLC39A6	SLIT2	SNAI2	SRC	TFF3	TGFB1	THBS1	TP53	TP73	TWIST1	VEGFA	XBP1

C

	1	2	3	4	5	6	7	8	9	10	11	12
A	ABCF2	ACTN4	ATAD2	CLVS1	DERL1	ETV1	GNAS	MRPL15	MYBL2	MYNN	NDRG1	PDCD10
B	PTP4A3	PUF60	RNF139	RSF1	SENP2	SS18L1	TBL1XR1	TPX2	UBE2C	ZFAT	ZFP64	Mref

Figure 4.2: Gene arrays displaying the 191 genes analyzed to generate gene expression profiles for patient samples. (A) Genes included in RT² Profiler PCR Array – Human Apoptosis. (B) Genes included in RT² Profiler PCR Array – Human Breast Cancer. (C) Genes included in qBiomarker Copy Number PCR Array – Human Ovarian Cancer. (Modified from Qiagen product manuals)

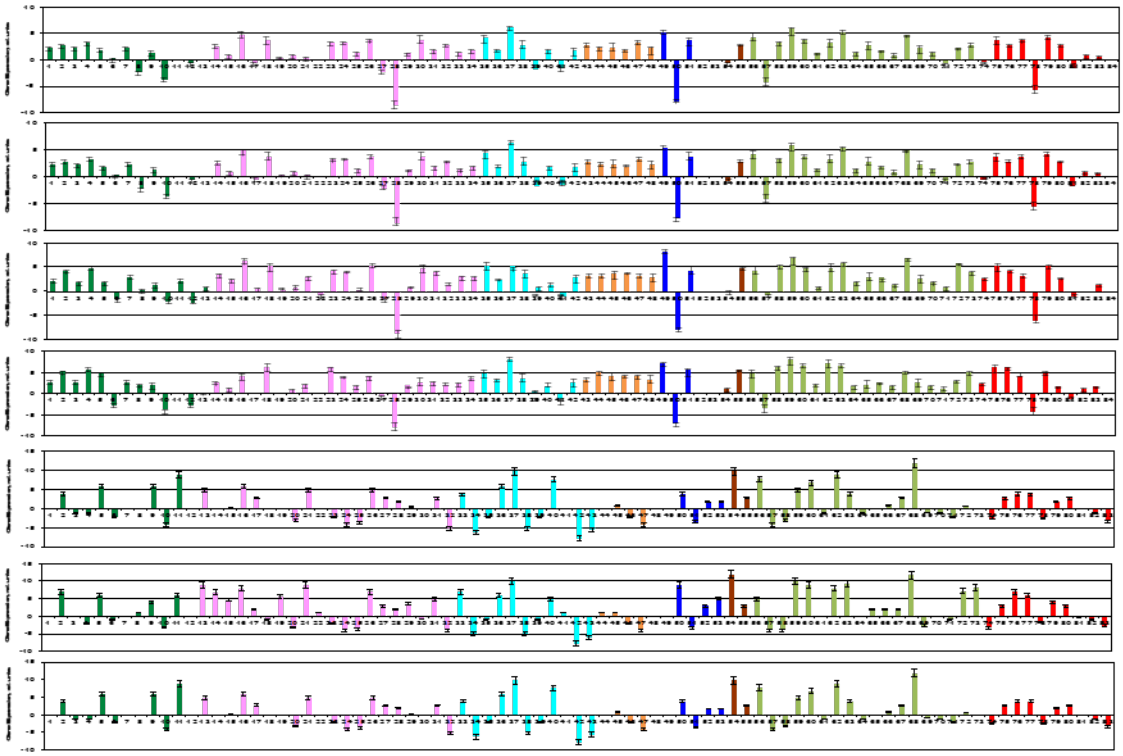

Figure 4.3: Gene expression profiles for seven ovarian cancer patients obtained from The Cancer Institute of New Jersey. These profiles were generated to contain the 84 selected genes selected for future patient analysis.

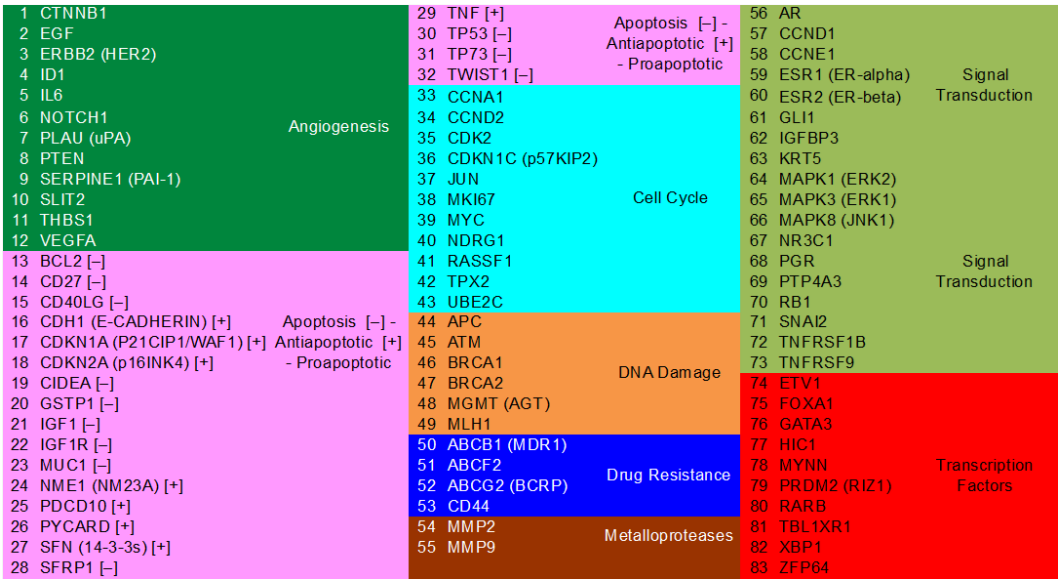

Figure 4.4: Compiled table containing the 84 selected genes to be used to analyze future patients. Genes have been categorized based on their general cellular functions, which includes angiogenesis, apoptosis regulation, cell cycle regulation, DNA damage repair, drug resistance, metalloproteases, signal transduction, and transcription factors.

5 Categorization and Optimization of Nanoparticle-Based Formulations for Delivering of Chemotherapeutic Drugs and Nucleic Acids

5.1 Introduction

The prosed co-therapy in this study utilized RNAi therapy and small molecule chemotherapy. For the RNAi therapy, siRNA macromolecules were used as the therapeutic agents. When naked siRNA is injected into systemic circulation, it has a number of problems that make it challenging to be effective in treating patients. First, siRNA has poor stability in the blood plasma. This is due to proteases that quickly degrade the molecules when they come into contact [158]. This mean most of them will be broken down way before they reach the desired site of action. Another issue with treating patients with naked siRNA is they have an extremely short half-life in the body due to their small molecular size. The siRNA molecules are quickly filtered into the urine by the kidneys. This quick elimination combined with their instability in blood plasma has been shown to give siRNA a half-life of roughly one minute inside the body. Not only that, there is one other property of nucleotide that give them no chance of being effective as therapeutic agents when naked siRNA is introduced to the body. All nucleotide have an anionic charge. The overall surface charge of cell membranes is also anionic. Consequently, naked siRNA cannot penetrate the cell membrane due electrostatic repulsion [156, 157]. Resulting in none of the siRNA internalizing into the cells to downregulate the expression of the target gene(s). All of these

challenges can be overcome by using nanoparticle DDSs. They can complex the siRNA, protect it from degradation, and help facilitate cellular internalization of these nucleotides [158].

Traditional chemotherapeutic agents fail to differentiate between the cancerous cells and normal healthy cells. Since these agents are designed to eliminate tumors by causing cell death, they will kill any cell they interact with inside the body. This indiscriminate destruction can cause damage to healthy non-target tissues and organs, leading to adverse side effects and toxicity issues in patients receiving the treatment [8]. The pharmaceutical industry has incorporated various DDS formulations to their pipeline to improve the efficacy of novel therapeutic agents and their existing FDA-approved products. As mentioned earlier, the reason DDSs have become popular is the fact that they can improve on the existing pharmacokinetic (PK) and pharmacodynamics (PD) properties of a therapeutic entity [12-16, 159]. Targeted delivery of conventional chemotherapeutics, specifically to cancer cells, can reduce off-target disposition of the chemotherapeutics and the adverse side effects that accompany this disposition. By exploiting overexpressed cell surface receptors, it is possible to increase the accumulation of chemotherapeutics at the desired site of action. Ligands that interact with the overexpressed receptors can be conjugated to a drug and have been shown to increase its delivery and internalization of specific cells [9, 128-132].

In the current study, we investigated two different types of nanoparticle DDSs; liposomes and dendrimers. We categorized multiple formulations of both DDSs and investigate which would be optimal for our proposed co-therapy. The work below describes and illustrates the properties of each formulation and which ones were chosen for further experimentation.

5.2 Materials and Methods

5.2.1 Materials

The following lipids: N-[1-(2,3-Dioleoyloxy)propyl]-N,N,N-trimethylammonium chloride (DOTAP), 1,2-dioleoyl-sn-glycero-3-phosphoethanolamine (DOPE), and 1,2-distearoyl-sn-glycero-3-phosphoethanolamine-N-[maleimide (polyethylene glycol)-2000] (ammonium salt) (DSPE-PEG(2000) Maleimide) were purchased from Avanti Polar Lipids (Alabaster, AL, USA). A synthetic analog of LHRH, Lys6-des-Gly10-Pro9-ethylamide (Gln-His-Trp-Ser-Tyr-DLys-Leu-Arg-Pro-NH-Et) was synthesized and purchased from American Peptide (Sunnyvale, GA, USA). 3-[4, 5-dimethylthiazole-2-yl]-2, 5-diphenyltetrazolium bromide (MTT Yellow), 4′, 6-Diamidine-2′-phenylindole dihydrochloride (DAPI), and Fluorescein 5(6)-isothiocyanate were purchased from Sigma-Aldrich Inc. (St. Louis, MO, USA). Sodium Dodecyl Sulfate (SDS) and N, N-Dimethylformamide (DMF) were purchased from Fisher Chemical (Fair Lane, NJ, USA). CELLSTAR® 96 Well Cell Culture Plates (Sterile, DNase/RNase Free) were purchased from Greiner

Bio-One GmbH (Monroe, NC, USA). The siGLO red was purchased from ThermoFisher Scientific Inc. (Waltham, MA, USA).

5.2.2 Preparation of Liposomes

Cationic liposomal formulations (Figure 5.1) were prepared using the thin-film hydration method as follows. The lipids were fully dissolved in ethanol. The contents were transferred to a round bottom flask and warmed to 42 0C. A thin film was formed using a rotary evaporator RotavaporTM R-210/R-215 (Buchi Corp., New Castle, DE, USA). Once the thin film was prepared, an appropriate buffer was added to ensure the final liposome concentration would be 20 mM during rehydration. Multilamellar large vesicle (MLV) liposomes were formed during the rehydration step. These vesicles were subjected to bath sonication using a ultrasonic bath from ThermoFisher Scientific Inc. (Waltham, MA, USA) for 40 minutes to disrupt the MLVs and form small unilamellar vesicle (SUV) liposomes.

Hydrophobic drugs (PTX and CIS) were dissolved with the lipids and were contained in the thin films formed during rotary evaporation. When the liposomes formed during rehydration, the drugs were retained in the double-lipid membranes of the liposomes. The water-soluble DOX was added to the rehydration buffer and was encapsulated when the liposomes were formed after the addition of the buffer.

5.2.3 Synthesis of Dendrimers

Several generations (G2, G3, G4, and G5) Poly(propylenimine) dendrimers (PPI) were purchased from Sigma-Aldrich (Milwaukee, WI). Sigma-Aldrich used the divergent method to synthesize the different dendrimers that we purchased from the company. These dendrimers were used in our studies without further purification.

5.2.4 Nanoparticle Morphology Imaging

Samples of the nanoparticles were imaged using atomic force microscopy (AFM). The images were obtained using a Nanoscope IIIA AFM (Digital Instruments, Santa Barbara, CA) as follows. A 125-μm long rectangular silicon cantilever/tip assembly with a spring constant of 40 Newton's per meters (N/m), resonance frequency of 315-352 kilohertz (kHz), and a tip radius of 5-10 nm was used for imaging the nanoparticle samples. Images were generated by the change in amplitude of the free oscillation of the cantilever/tip assembly as it interacted with each sample. The height differences detected by the instrument were indicated by changes of the color generated (lighter regions represent an increase in height) during imaging.

5.2.5 Nanoparticle Size and Zeta Potential

Nanoparticle aliquots were diluted in deionized (DI) water for measurements. Samples volumes of 1 mL were loaded into folded capillary cells designed by Malvern for use in their instruments. Both the size and zeta potential for the liposomal formulations were measured using the Zetatizer Nano-ZS (Malvern Panalytical Ltd., UK). The instrument uses their patented Non-Invasive Back Scattering (NIBS) technology to measure particle size. The technology is a form of dynamic light scattering that measures particles using a diode laser wavelength of 633 nm and the scattered light is captured with a detector with a backscatter angle of 1750. Zeta potential was measured using Malvern's patented M3 – Phase Analysis Light Scattering (PALS) technology.

5.2.6 Nanoparticle Cytotoxicity

Nanoparticle cytotoxicity was determined using the colorimetric 3-[4, 5-dimethylthiazole-2-yl]-2, 5-diphenyltetrazolium bromide (MTT) assay modified protocol as follows. Patient isolate cells were grown to confluence in cell culture flasks and collected as mentioned earlier (specific aim 1). Once the cells were pelleted by centrifugation, they were suspended in DPBS. Cell samples were then counted using a ScepterTM handheld automated cell counter (Millipore Corp., Billerica, MA, USA). Cell seeding densities were appropriately determined for each sample. The samples were seeded into 96-well microtiter plates and left

to incubate for one day. The following day, the nanoparticles were prepared at different concentrations using serial dilutions in media, added to the wells suitably, and left to incubate for 24 hours. Next, the media and nanoparticles were aspirated. Media mixed with MTT yellow were added to the wells and incubated for three hours. While the cells incubated, a MTT clear solution, containing dimethylformamide (DMF) and sodium dodecyl sulfate (SDS) dissolved in DI water, was prepared to dissolve the insoluble formazan crystals that formed during incubation. Once dissolution was complete, the microtiter plates were measured with the Nanoquant Infinite m200 (Tecan Trading AG, Switzerland) using a measurement wavelength of 570 nm and reference wavelength of 650 nm. Cell viability was calculated by dividing the experimental measurement by the reference measurement ([experimental ÷ control] *100).

5.2.7 Evaluate Complex Formation between Nanoparticles and Short Interfering RNA (siRNA)

To determine an optimal complex ratio between the nanoparticles and siRNA when formulating the treatments conducted later in our study, complexes were prepared in DI water at Nitrogen:Phosphate (N:P) ratios that ranged from 0 (naked siRNA) to three relative units. The nanoparticles were incubated with the siRNA for one hour one a rotator to form the complexes. After allowing the complexes to form, the samples were further diluted in DPBS and subjected agarose gel electrophoresis. The samples were loaded into a 4% agarose gel

and exposed to 100 volts (V) in Tris-Borate-EDTA buffer for one hour. Afterwards, ethidium bromide was added to label any naked siRNA that had not complexed with the nanoparticles. The labeled siRNA was imaged under ultraviolet (UV) light using a Gel Logic 440 Imaging System (Eastman Kodak Co.).

5.2.8 Cellular Internalization of Nanoparticle Complexes

To determine cellular internalization of the nanoparticle complexes, fluorescently-labeled molecular probes were incorporated into the DDS formulations. Cationic Liposomes were prepared with 5(6)-isothiocyanate (fluorescein, green fluorescence). These liposomes were placed on a rotator for one hour with fluorophore-labeled siRNA (siGLO Red, red fluorescence) to form liposome-siRNA complexes. Primary tumor isolate cultures were incubated with the fluorophore-labeled nanoparticle complexes for 24 hours. After this incubation period, media containing the fluorophore-labeled nanoparticle complexes was aspirated and the cells were washed three times with DPBS. The cells were then incubated for 20 minutes with 4′, 6-diamidino-2-phenylindole (DAPI, blue fluorescence) to stain and fluorescently label cell nuclei in the culture. Excess DAPI was removed by washing the cells five times with DPBS. A Leica G-STED SP8 confocal microscope (Leica Microsystems) was utilized to capture fluorescence images of each fluorophore, overlay image the fluorophores, and z-sections of the prepared cells.

5.2.9 Statistical Analysis

Statistical analysis was performed on the obtained data using single factor analysis of variants (ANOVA) and presented the results as the mean value ± standard deviation from three independent measurements. Data sets were analyzed for significance using t-tests considered P values less than 0.05 to be statistically significant.

5.3 Results

5.3.1 Properties of Liposomal Formulations

The properties of the three liposomal formulations analyzed in this study can be found in Figure 5.2. As the ratio of DOPE:DOTAP increased, the size of the particles increased as well. However, the size differences between the formulations were not significantly different. Also, the polydispersion index remained relatively stable between the three formulations. The zeta potential did significantly change between the formulations. The zeta potential DOTAP + DSPE-PEG-LHRHR (96:4 molar ratio) liposomes were measured at 84.37 ± 3.85 mV. The DOTAP + DOPE + DSPE-PEG-LHRHR (48:48:4 molar ratio) liposomes had a zeta potential measured at 50.90 ± 1.10 mV. Lastly, DOTAP + DOPE +

DSPE-PEG-LHRHR (32:64:4 molar ratio) liposomes had a zeta potential measured at 30.63 ± 1.77 mV. The Cytotoxicity for each of the formulations was significantly different from one another (Figure 5.3). As the zeta potential increased, the cytotoxicity did as well.

5.3.2 Properties of Dendrimer Formulations

The morphology of the dendrimers changed quite a bit from G2 to G5 (Figure 5.4). G2 PPI dendrimers has a spindled and flat shape to them and as the generations increased, the morphology became more spherical. G4 PPI dendrimers exhibited the greatest level of siRNA internalization among the different generations. This is further validated since the suppression of CD44 expression levels was greatest in cells treat with G4 PPI dendrimers compared to the other generation dendrimers (Figure 5.5). Cytotoxicity of the PPI dendrimers remained relatively constant between G2 and G3, but increased significantly for G4 and G5 (Figure 5.6). G5 had the highest cytotoxicity between all of the different generation PPI dendrimers.

5.4 Discussion

To begin with the liposomes, we evaluated three cationic formulations. Formulation 1 (DOTAP + DSPE-PEG-LHRHR) formed the smallest particles compared to the other two formulations. However, this formulation displayed

significantly highest levels of cytotoxicity. The cytotoxicity was so high that in some of the highest treatment concentrations, the particles complexed with certain components in the media and crashed out of solution. A white cloudy precipitate formed and all of the cells were killed when incubated with the solution containing it. Obviously, this high level of cytotoxicity would be a problem when treating cells with our co-therapy and the formulation was deemed too toxic for use in further experiments. Formulation 2 (DOTAP + DOPE + DSPE-PEG-LHRHR – 48:48:4 molar ratio) showed significant improvements over formulation 1. The size of the particles increased, but not significantly. The cytotoxicity of formulation 2 improved significantly and quite drastically compared to formulation 1. Finally, formulation 3 (DOTAP + DOPE + DSPE-PEG-LHRHR – 32:64:4 molar ratio) further improved the particle cytotoxicity, while maintaining a statistically similar particle size compared to the other two formulations. Therefore, we deemed formulation 3 the optimal liposomal formulation to continue using in our study.

There were 4 different generation dendrimers investigated in this specific aim (G2, G3, G4, and G5). Both G2 and G3 were discovered to have a spindled and branched rod-like morphology when imaged using AFM. This morphology not only contributed poor siRNA complexation, but it is also the most likely reason why the particles did not internalized into the cells efficiently. While the G2 and G3 dendrimers showed similar levels of cytotoxicity, which was significantly lower than the G4 and G5 dendrimers, the poor levels of cellular transfection and

delivery of the siRNA made them poor choices to use in further experimentations in our study. The G4 and G5 dendrimers both had a spherical morphology when imaged using AFM. However, G5 was significantly more cytotoxic than the G4 dendrimers. Not only this, the G4 dendrimers exhibited the highest levels of CD44 gene expression knockdown compared to the other three generations. As a result, the G5 dendrimers were deemed inadequate compared to G4.

5.5 Conclusions

The liposomal formulation 3 and G4 dendrimers were considered to be the optimal formulations out of their counterparts. It appears that surface charge does play a role in cytotoxicity levels as demonstrated by the data collected. As the zeta potential of the liposomes decreased, the level of cytotoxicity decreased with it. The same can be concluded with the dendrimers. When dendrimers undergo further reaction to form the next generation. This means an increased amount of the amino functional groups on the PPI dendrimers would increase exponentially and this would result in a higher cationic surface charge of the nanoparticle. All in all, we needed to find a balance between lipid in the liposomal formulation and the generation limit in the dendrimers to optimized nucleotide complexation while balancing optimal cellular transfection levels for gene expression knockdown.

A

N-[1-(2,3-Dioleoyloxy)propyl]-N,N,N-trimethylammonium chloride (DOTAP)

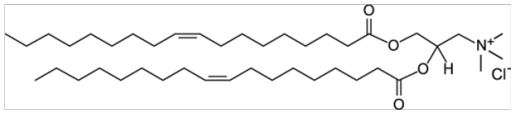

1,2-dioleoyl-sn-glycero-3-phosphoethanolamine (DOPE)

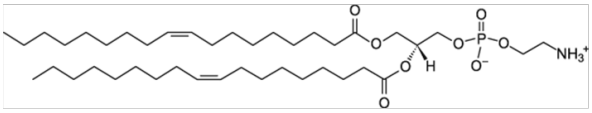

1,2-distearoyl-sn-glycero-3-phosphoethanolamine-N-[maleimide (polyethylene glycol)-2000] (ammonium salt) (DSPE-PEG(2000) Maleimide)

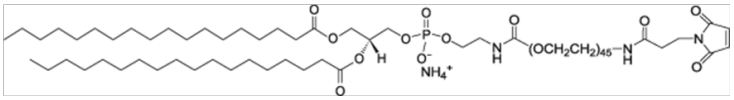

B

Formulation No.	Formulation Components (Molar ratios)
1	DOTAP + PEG-DSPE-LHRH (96:4)
2	DOTAP + DOPE + PEG-DSPE-LHRH (48:48:4)
3	DOTAP + DOPE + PEG-DSPE-LHRH (32:64:4)

Figure 5.1: Overview of liposome preparation. (A) Lipids included in the liposome formulations. (B) The three liposome formulations investigated.

	Liposome Formulation	Mean Particle size(nm)	Polydispersion index(PDI)	Zeta Potential(mV)
1	DOTAP + DSPE-PEG-LHRH (96:4)	94.31 ±9.03	0.255 ±0.003	84.37 ±3.85
2	DOTAP + DOPE + DSPE-PEG-LHRH (48:48:4)	98.72 ±3.05	0.197 ±0.016	50.90 ±1.10
3	DOTAP + DOPE + DSPE-PEG-LHRH (32:64:4)	103.93 ±1.68	0.245 ±0.021	30.63 ±1.77

Figure 5.2: Properties of the three liposome formulations investigated in this study.

Formulation No.	Formulation Components (Molar ratios)
1	DOTAP + PEG-DSPE-LHRH (96:4)
2	DOTAP + DOPE + PEG-DSPE-LHRH (48:48:4)
3	DOTAP + DOPE + PEG-DSPE-LHRH (32:64:4)

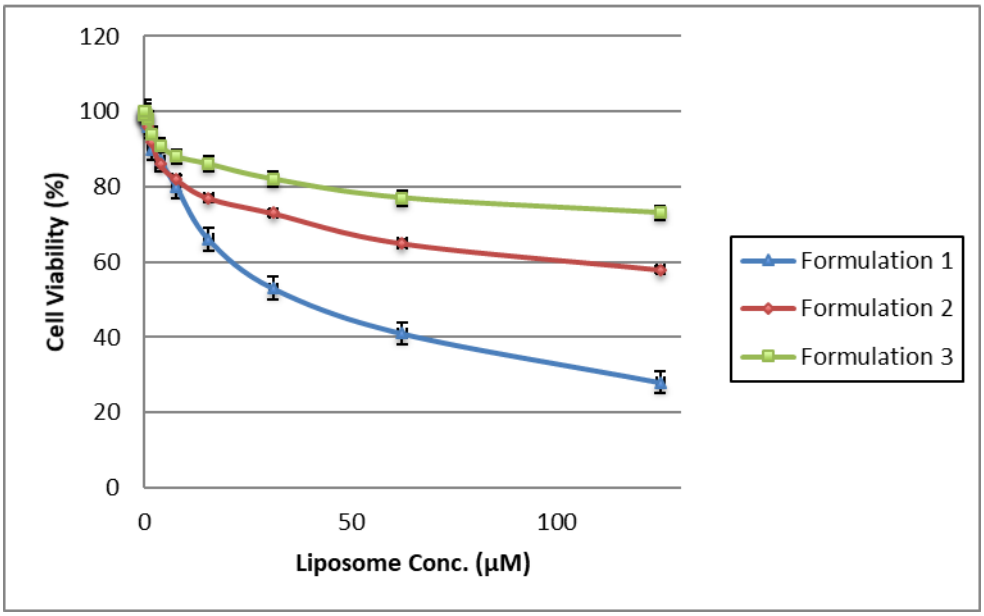

Figure 5.3: MTT cytotoxicity data for liposome formulations investigated in this study.

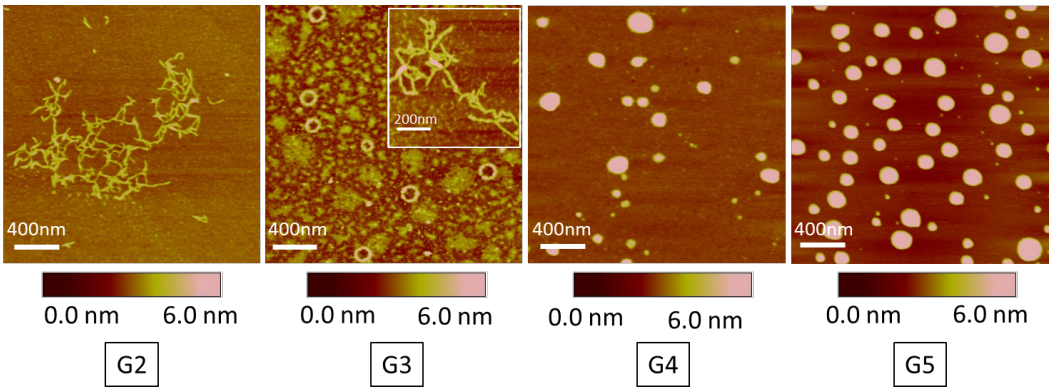

Figure 5.4: Morphology of different generation (G) PPI dendrimers obtained using ATM imaging. (Modified from Ref. [207])

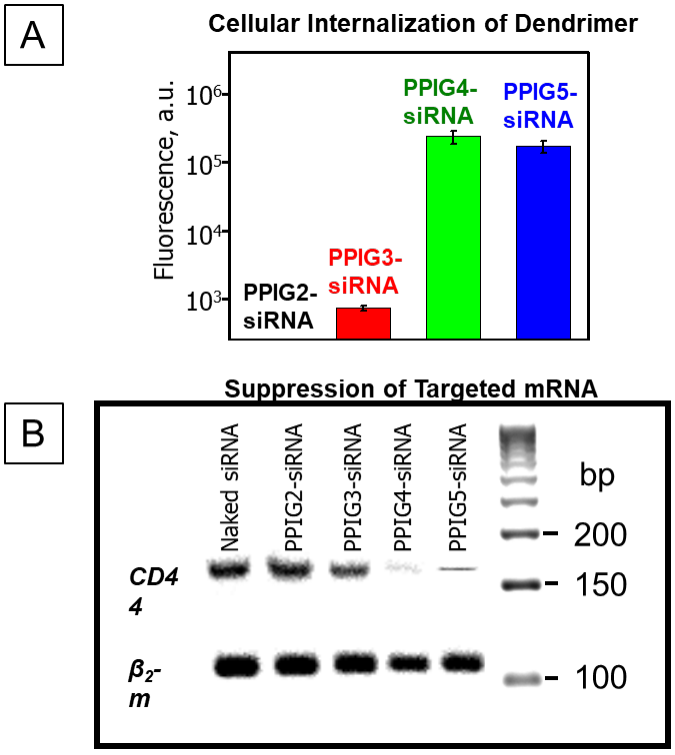

Figure 5.5: Efficiency of dendrimer-mediated cellular transfection of siRNA. (A) Cellular internalization of fluorophore-labeled siRNA using fluorescent microscopy. (B) Gel electrophoresis image of CD44 suppression after dendrimer-mediated cellular internalization of CD44 siRNA. (Modified from Ref. [207])

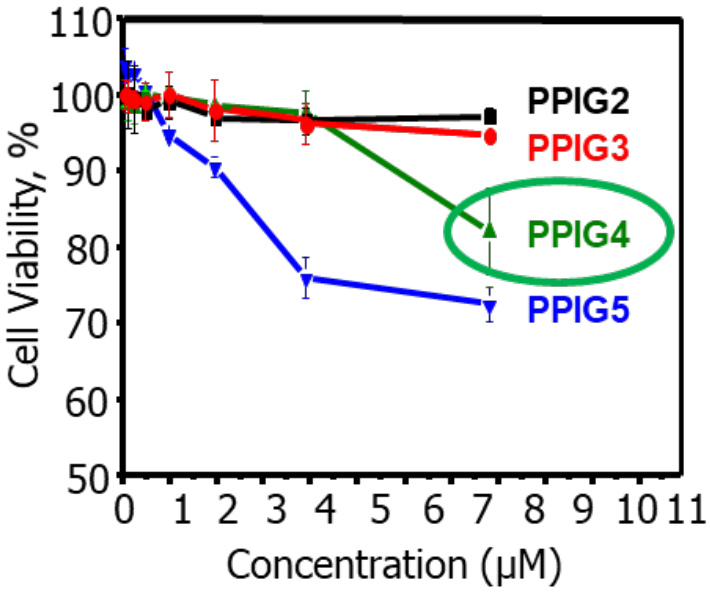

Figure 5.6: MTT cytotoxicity of different generation (G) PPI dendrimers obtained using ATM imaging. (Modified from Ref. [207])

6 Evaluation of the Therapeutic Efficiency of the Various Targeted Nanotechnology-Based Chemo/siRNA Combinatorial Delivery Systems

6.1 Introduction

The current 5-year survival rate for patients with advanced-stage ovarian cancer is a meager 30% [5-7]. This can be accredited to the fact that the disease has become highly invasive and multidrug resistant by the time it has been diagnosed in most patients. Most treatments can help reduce and possible eliminate the primary tumor, but a lot of patients have metastatic recurrent tumors that develop after treatment ends [205, 206].

As a result, targeted therapeutics has become one of the main focuses in oncology research to improve the issues with toxicity in patients. Targeted therapeutics exploit abnormalities resulting from disease progression and are not present in healthy cells, tissues and organs [9-11]. As mentioned earlier, nanoparticle drug delivery systems (DDSs) have demonstrated great potential for precision treatment of cancer. By conjugating a certain ligand to a DDS, specifically one that can interact with a cell surface receptor expressed in the diseased states, it acquires the ability to target those cells and produces higher concentrations at the target site of action [20-24].

Here, we investigated the therapeutic efficacy of our proposed co-therapy system using multiple drugs. We already analyzed patient gene expression profiles and optimized our nanoparticle DDSs. We evaluated the co-therapy using our liposomal DDS *in vitro* and are current developing an animal model for evaluating its efficacy *in vivo*. Based on previous work in our lab [141, 156, 207, 208], we knew the potential for our dendrimer DDS *in vitro* and proceeded to investigate it's efficacy in animal models for *in vivo* evaluation.

6.2 Materials and Methods

6.2.1 Materials

The following lipids: N-[1-(2,3-Dioleoyloxy)propyl]-N,N,N-trimethylammonium chloride (DOTAP), 1,2-dioleoyl-sn-glycero-3-phosphoethanolamine (DOPE), and 1,2-distearoyl-sn-glycero-3-phosphoethanolamine-N-[maleimide (polyethylene glycol)-2000] (ammonium salt) (DSPE-PEG(2000) Maleimide) were purchased from Avanti Polar Lipids (Alabaster, AL, USA). A synthetic analog of LHRH, Lys6-des-Gly10-Pro9-ethylamide (Gln-His-Trp-Ser-Tyr-DLys-Leu-Arg-Pro-NH-Et) was synthesized and purchased from Americn Peptide (Sunnyvale, GA, USA). 3-[4, 5-dimethylthiazole-2-yl]-2, 5-diphenyltetrazolium bromide (MTT Yellow), 4′, 6-Diamidine-2′-phenylindole was purchased from Sigma-Aldrich Inc. (St. Louis, MO, USA). Sodium Dodecyl Sulfate (SDS) and N, N-Dimethylformamide (DMF) were purchased from Fisher Chemical (Fair Lane, NJ, USA). CELLSTAR® 96

Well Cell Culture Plates (Sterile, DNase/RNase Free) were purchased from Greiner Bio-One GmbH (Monroe, NC, USA). Female athymic nu/nu mice were purchased from Taconic (Hudson, NY, USA). All of the siRNA used for our RNAi therapy were purchased from Qiagen (Hilden, Germany).

6.2.2 Gene Expression Knockdown Efficiency

For patients we evaluated the co-therapies in this study, we targeted five genes. The five genes were: BCL2, MDR1, CD44, MMP9, and PGR. For the in vitro analysis of targeted gene expression knockdown efficiency, patent isolate cultures were grown to 80% confluence in culture flasks. Once the samples were grown, nanoparticle-siRNA complexes were formed, mixed with media to dilute the complexes to the appropriate concentration and incubated with the cells for 24 hours. At the same time, identical sample culture were incubated with media only and served as control samples. Cells were collected, lysed, the total RNA was isolated/purified, and reverse transcribed as mentioned in specific aim 1. Sample cDNA was prepared for qRT-PCR as mentioned earlier, but was added to the customized 84 gene assay we designed based on the results we obtained when profiling the gene expression profiles of patient samples performed in specific aim 1. The qRT-PCR reactions were run for all samples as previously mentioned as well. Both the control and experimental samples were compared using the ΔΔCT method. For the in vivo experiments, the remaining tumor tissues were excised from the mice and homogenized. RNA

extraction/purification, RT reaction, and qRT-PCR was carried out using the same protocol as the in vitro experiments.

6.2.3 *In Vitro* cytotoxicity

Cytotoxicity of our various treatments were determined using the colorimetric 3-[4, 5-dimethylthiazole-2-yl]-2, 5-diphenyltetrazolium bromide (MTT) assay modified protocol as follows. Patient isolate cells were grown to confluence in cell culture flasks and collected as mentioned earlier (specific aim 1). Once the cells were pelleted by centrifugation, they were suspended in DPBS. Cell samples were then counted using a ScepterTM handheld automated cell counter (Millipore Corp., Billerica, MA, USA). Cell seeding densities were appropriately determined for each sample. The samples were seeded into 96-well microtiter plates and left to incubate for one day. The following day, the nanoparticles were prepared at different concentrations using serial dilutions in media, added to the wells suitably, and left to incubate for 24 hours. Next, the media and nanoparticles were aspirated. Media mixed with MTT yellow were added to the wells and incubated for three hours. While the cells incubated, a MTT clear solution, containing dimethylformamide (DMF) and sodium dodecyl sulfate (SDS) dissolved in DI water, was prepared to dissolve the insoluble formazan crystals that formed during incubation. Once dissolution was complete, the microtiter plates were measured with the Nanoquant Infinite m200 (Tecan Trading AG, Switzerland) using a measurement wavelength of 570 nm and reference

wavelength of 650 nm. Cell viability was calculated by dividing the experimental measurement by the reference measurement ([experimental ÷ control] *100).

6.2.4 Animal Model and In Vivo Antitumor Activity

To create an animal model for the study, a patient sample was subcutaneously injected into the flanks of female athymic nu/nu mice (Taconic, Hudson, NY, USA). Once the tumors grew to a size of about 0.4 cm3, mice were treated 8 times twice per week for 4 weeks with one of our treatment formulations. The development of the primary tumor and metastases were monitored using IVIS Lumina Imaging System (Xenogen, Alameda, CA, USA) and Vevo 2100 Ultrasound System (VisualSonics, Toronto, Canada). During the treatment course, a caliper was utilized to measure the size of the primary tumor at various time points and the weight of the animals were evaluated daily. When the experiment was finished, the primary tumor was excised and the mass was measured. Changes in the tumor size were used as a marker to determine antitumor activity in the mice.

6.2.5 Statistical Analysis

Statistical analysis was performed on the obtained data using single factor analysis of variants (ANOVA) and presented the results as the mean value ± standard deviation from three independent measurements. Data sets were

analyzed for significance using t-tests considered P values less than 0.05 to be statistically significant.

6.2.6 Veterinary Care

Rutgers University Laboratory Animal Services provided veterinary care for all mice included in this study. All of the in vivo procedures were conducted according to the guidelines set by the National Institute of Health Guide and of Animals as well as the Institutional Animal Care and Use Committee at Rutgers University, NJ.

6.3 Results

6.3.1 Gene Expression Knockdown Efficiency and Protein Levels After Chemo/siRNA Combinatorial Therapeutic Treatment

The expression knockdown of our targeted genes in our different therapies was efficient. The control samples showed gene expression was relatively constant, while the treatment samples showed a significant decrease in gene expression. Knockdown efficiencies were observed to range from roughly 35% to as high as 85% for patients 1 and 2 after being treated using our liposome DDS (Figure 6.1). The gene expression knockdown translated into decrease protein levels in

the treatment samples as well (Figure 6.2). Similar levels of gene knockdown were observed *in vivo* after treatment (Figure 6.3).

6.3.2 *In Vitro* cytotoxicity of Chemo/siRNA Combinatorial Delivery Systems

Primary tumor isolates cultures that were treated with one of the co-therapies showed a significant increase in chemotherapeutic efficacy. Cells treated with a co-therapy formulated with CIS resulted in an IC50 of 4.85 μM for patient 1 and 15.09 μM for patient 2. The CIS monotherapy, resulted in an IC50 of 49.81 μM for patient 1 and 105.62 μM for patient 2 (Figure 6.4). The co-therapy formulated with DOX resulted in an IC50 of 9.65 Mm for patient 1 and 39.94 μM for patient 2. The DOX monotherapy resulted in an IC50 of 92.98 μM for patient 1 and 101.85 μM for patient 2 (Figure 6.5). The co-therapy formulated with PTX resulted in an IC50 of 74.73 μM for patient 1 and 89.53 μM for patient 2. The PTX monotherapy resulted in an IC50 of 10.93 μM for patient 1 and 14.59 μM for patient 2 (Figure 6.6).

6.3.3 *In Vivo* Antitumor Activity of Chemo/siRNA Combinatorial Delivery Systems

Mice subjects treated with saline, non-targeted empty dendrimers, targeted empty dendrimers, and non-targeted dendrimers complexed with scrambled

siRNA did not influence the tumor growth in the mice and all showed similar growth patterns. Mice treated with free PTX showed some response to the treatment, but the tumor size still grew overall. The PTX conjugated dendrimers showed even more treatment response, but there was still an increase of the overall tumor size over the course of the experiment. Mice treated with targeted dendrimers complexed with siRNA showed good efficacy for decreasing the growth rate of the tumor and only resulted in a slight increase in the size of the tumor. Finally, mice that were treated with targeted PTX conjugated dendrimers and dendrimers complexed with siRNA resulted in a steady decrease in tumor volume over the experiment and by the end of the experiment, there was a small amount of primary tumor remaining these mice (Figure 6.7-A). Also, intraperitoneal metastases were detected in all treatments expect for the targeted PTX conjugated dendrimers and dendrimers complexed with siRNA treatment (Figure 6.7-B).

6.4 Discussion

The present investigation into our nanoparticle-based co-therapies appear to have excellent potential for clinical application. The liposome-delivered co-therapies demonstrated significant increases in therapeutic efficacy compared to their corresponding monotherapy. Our *in vitro* cytotoxicity assays resulted in IC_{50} values that were approximately one-tenth for both DOX and CIS co-therapies compared to their corresponding monotherapy for patient 1. Therefore, both the

DOX and CIS co-therapies resulted in roughly a 10-fold increase in therapeutic efficacy. Similar results were observed for the CIS co-therapy for patient 2, but the IC_{50} DOX co-therapy was only a little more than half than the DOX monotherapy (Figures 6.3 & 6.4). Perhaps targeting other efflux protein using RNAi would improve the results. The PTX co-therapy efficacy was significantly higher than the PTX monotherapy for both patients. However, the PTX co-therapy did not perform as well as the CIS co-therapy for both patients and the DOX co-therapy for patient 1. The IC_{50} of the PTX was about 15% of the PTX monotherapy (Figure 6.5). Therefore, the PTX co-therapy demonstrated approximately 6-fold increase in therapeutic efficacy. This is still a significant outcome, but not quite as much when compared to the other two co-therapies.

The PPI co-therapy we investigated could be extremely promising in the clinic. The animal model treated with the targeted-PPI PTX/RNAi co-therapy showed tumor size reduction over the course of the treatment. By the end of the experiment, the tumor was almost completely eliminated in the mice. Even more amazing, the mice treated with the co-therapy had no intraperitoneal metastases detected unlike all of the other treatments investigated in the experiments (Figure 6.6). Thus, this co-therapy was extremely efficient in reducing and destroying the primary tumor that developed and prevent the tumor from metastasizing within the animal model.

For both nanoparticle-based co-therapies, we observed efficient gene expression knockdown for the five target genes (Figure 6.1). We not only chose the genes because they were highly overexpressed in our patient samples, but due to their cellular functions as well. BCL2 is a known apoptosis suppressor and it contributes to tumor resilience [210]. MDR1 is a cell-surface efflux pump protein and overexpression has been known to cause multidrug resistant cancers [211]. CD44 is involved in cell adhesion, migration, and can cause changes to a tumor microenvironment. Therefore, overexpression can lead to cancer progression and metastasis [212]. MMP9 is involved in proteolysis of extracellular matrices and can aid in tumor metastasis [213]. PGR is involved in regulating certain gene expression pathways involved in cellular proliferation and differentiation. Thus, it can cause tumor growth and disease progression when overexpressed [214]. It was proposed that downregulating the expression of these genes could make the tumor more susceptible to currently used small molecule chemotherapeutic drugs for ovarian cancer. We believe that this hypothesis was correct and attributed to the high levels of therapeutic efficacy observed in all of the co-therapies investigated in the study.

6.5 Conclusions

The proposed chemo/RNAi therapy concept we investigated appears as though it might have potential for treating ovarian cancer patients in the clinic. The dendrimer DDS exhibited high levels of efficacy in our animal model. The

liposomal DDS also showed increases in therapeutic efficacy for the three chemotherapeutic drugs included in the study. Obviously further experiments in animal models will be needed to validate the *in vitro* results we obtained, but we feel there will a similar outcome as the targeted-PPI PTX/RNAi co-therapy.

Figure 6.1: Gene expression knockdown efficiency of liposome DDS.

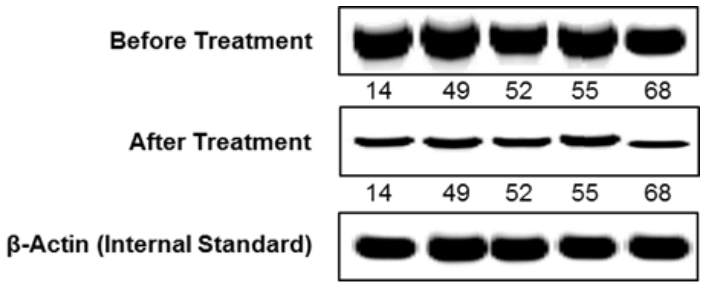

14. BCL2
49. ABCB1 (MDR1)
52. CD44
55. MMP9
68. PGR

Figure 6.2: Protein levels of target genes before and after treatment with our liposome DDS.

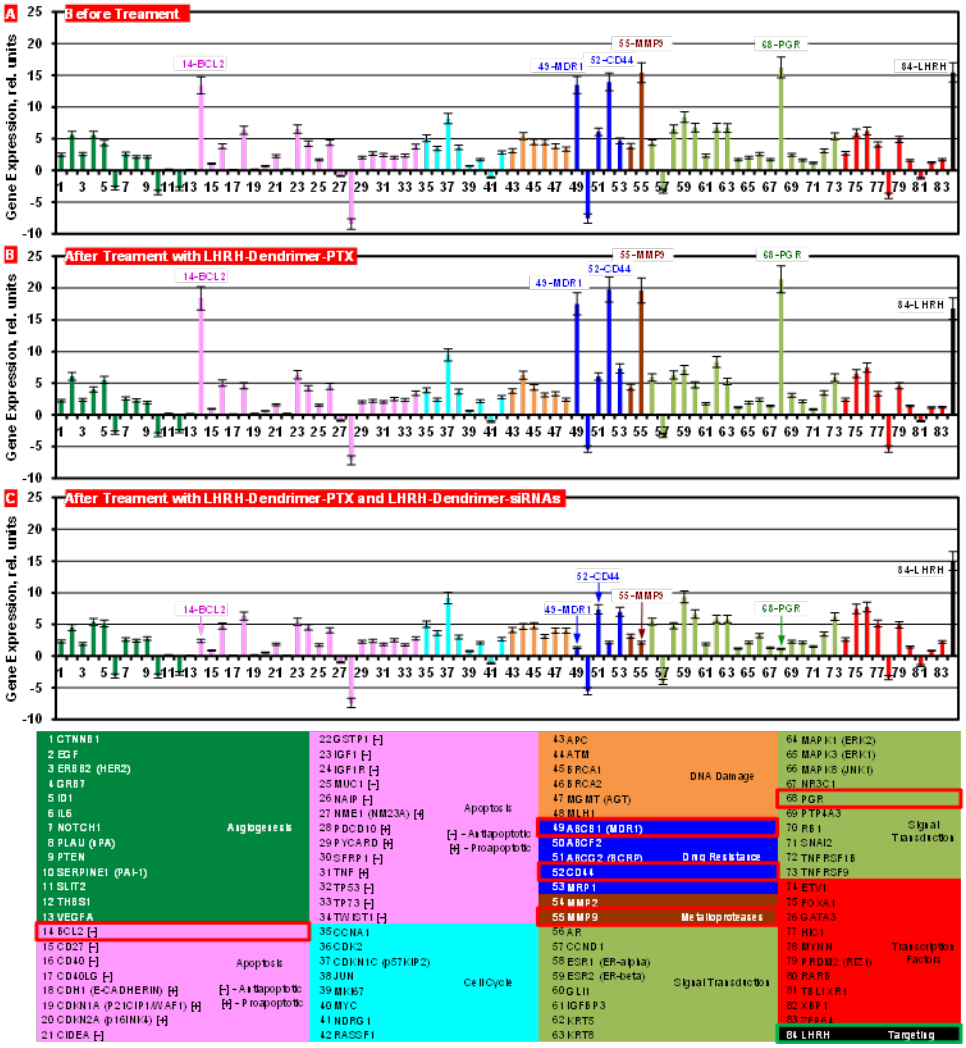

Figure 6.3: Gene expression knockdown efficiency of our dendrimer DDS in our animal model. (Reproduced from Ref. [209])

A

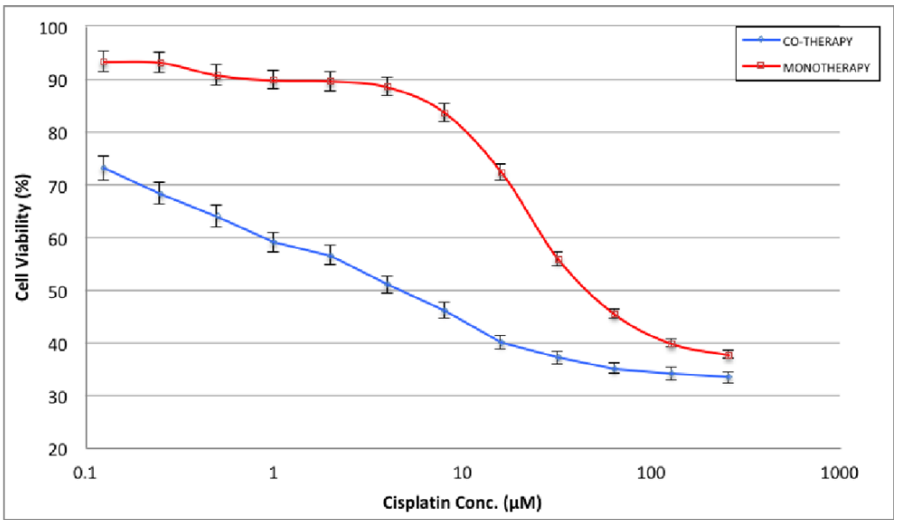

B

Treatment	IC50 (µM)	
	Patient 1	Patient 2
CIS Only	49.81	105.62
CIS + Lipoplex	4.85	15.09

Figure 6.4: MTT cytotoxicity data for CIS co-therapy vs. CIS Monotherapy. (A) Graphical depiction of cytotoxicity curve observed in patient 1. (B) Table compiling the IC_{50} results obtained for both patients.

A

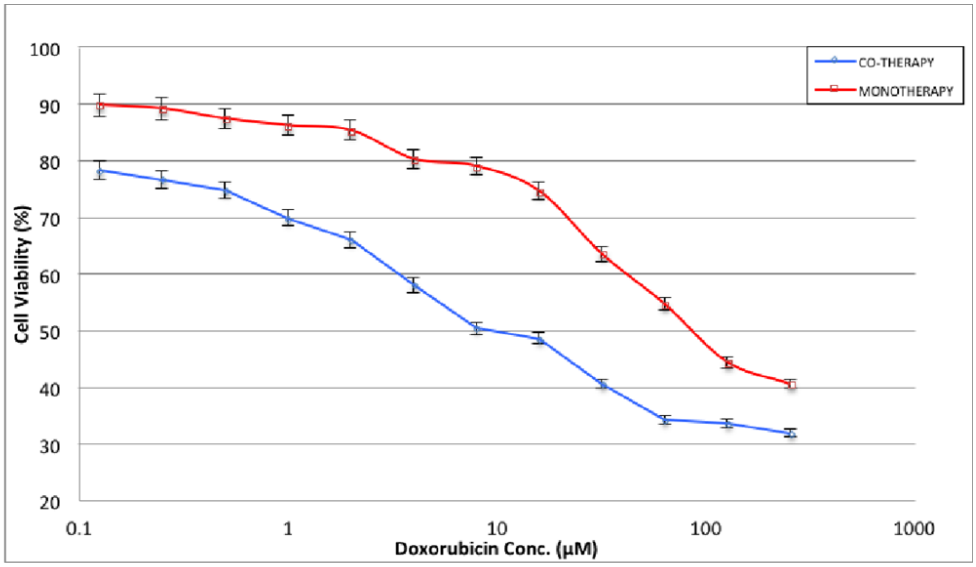

B

Treatment	IC50 (µM)	
	Patient 1	Patient 2
DOX Only	92.98	101.85
DOX + Lipoplex*	9.65	39.94

Figure 6.5: MTT cytotoxicity data for DOX co-therapy vs. DOX Monotherapy. (A) Graphical depiction of cytotoxicity curve observed in patient 1. (B) Table compiling the IC_{50} results obtained for both patients.

A

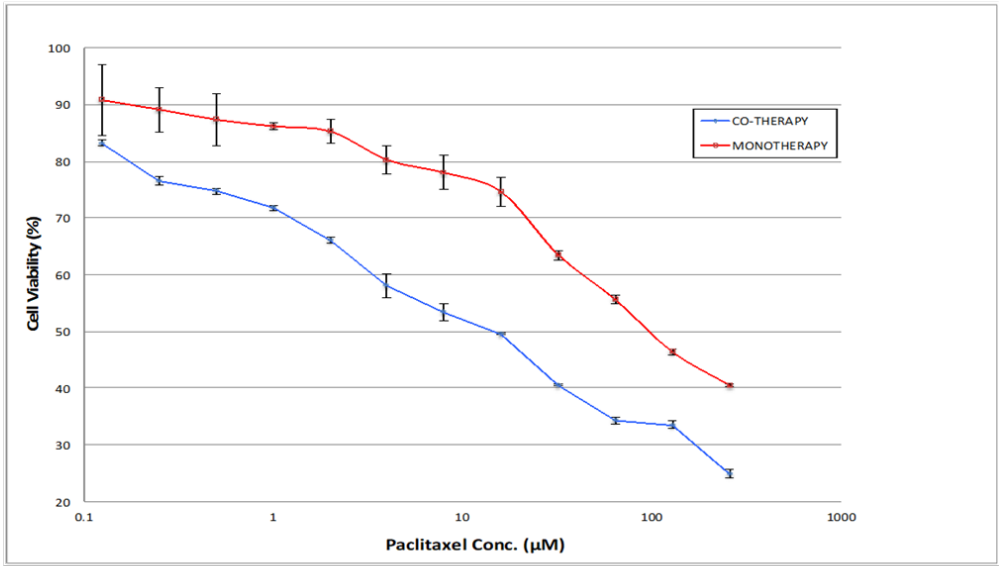

B

Treatment	IC50 (µM)	
	Patient 1	Patient 2
PTX Only	74.73	89.83
PTX + Lipoplex	10.93	14.59

Figure 6.6: MTT cytotoxicity data for PTX co-therapy vs. PTX Monotherapy. (A) Graphical depiction of cytotoxicity curve observed in patient 1. (B) Table compiling the IC_{50} results obtained for both patients.

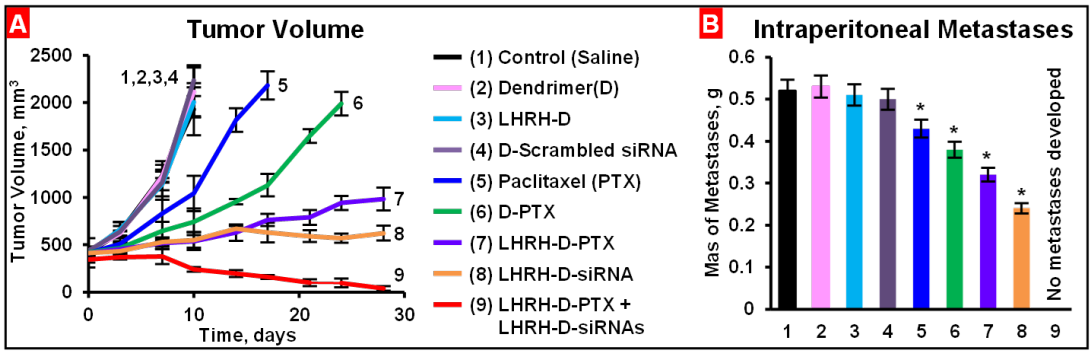

Figure 6.7: Anti-tumor effects in our animal model. (A) Tumor volume over the course of the experiment for various treatments. (B) Detection and evaluation of intraperitoneal metastasis formation. (Reproduced from Ref. [209])

7 References

[1] P.K. B.W. Stewart, World Cancer Report, World Health Organizaton, Lyon, 2003.

[2] R.L. Siegel, K.D. Miller, A. Jemal, Cancer statistics, 2019, CA Cancer J Clin, 69 (2019) 7-34.

[3] B. Spear, M. Heath-Chiozzi, J. Huff, Clinical application of pharmacogenetics, Trends Mol Med, 7 (2001) 201-204.

[4] J. Ferlay, I. Soerjomataram, R. Dikshit, S. Eser, C. Mathers, M. Rebelo, D.M. Parkin, D. Forman, F. Bray, Cancer incidence and mortality worldwide: sources, methods and major patterns in GLOBOCAN 2012, Int J Cancer, 136 (2015) E359-386.

[5] A.C. Society, Cancer Facts and Figures 2015, American Cancer Society, Atlanta, 2015.

[6] S.A. Cannistra, Cancer of the Ovary, The New England Jounral of Medicine, 351 (2004) 2519-2529.

[7] D. Lane, I. Matte, C. Rancourt, A. Piche, The prosurvival activity of ascites against TRAIL is associated with a shorter disease-free interval in patients with ovarian cancer, J Ovarian Res, 3 (2010) 1.

[8] R. Sinha, G.J. Kim, S. Nie, D.M. Shin, Nanotechnology in cancer therapeutics: bioconjugated nanoparticles for drug delivery, Mol Cancer Ther, 5 (2006) 1909-1917.

[9] J. Lopez, S. Banerjee, S.B. Kaye, New developments in the treatment of ovarian cancer--future perspectives, Ann Oncol, 24 Suppl 10 (2013) x69-x76.

[10] S. Narod, Can advanced-stage ovarian cancer be cured?, Nature Reviews Clinical Oncology, 13 (2016) 255-261.

[11] M. Haemmerle, J. Bottsford-Miller, S. Pradeep, M.L. Taylor, H.J. Choi, J.M. Hansen, H.J. Dalton, R.L. Stone, M.S. Cho, A.M. Nick, A.S. Nagaraja, T. Gutschner, K.M. Gharpure, L.S. Mangala, R. Rupaimoole, H.D. Han, B. Zand, G.N. Armaiz-Pena, S.Y. Wu, C.V. Pecot, A.R. Burns, G. Lopez-Berestein, V. Afshar-Kharghan, A.K. Sood, FAK regulates platelet extravasation and tumor growth after antiangiogenic therapy withdrawal, J Clin Invest, 126 (2016) 1885-1896.

[12] K. Cho, X. Wang, S. Nie, Z.G. Chen, D.M. Shin, Therapeutic nanoparticles for drug delivery in cancer, Clin Cancer Res, 14 (2008) 1310-1316.

[13] O.C. Farokhzad, R. Langer, Impact of Nanotechnology on Drug Delivery, American Chemical Society Nano, 3 (2009) 16-20.

[14] C. Fang, M. Zhang, Nanoparticle-based theragnostics: Integrating diagnostic and therapeutic potentials in nanomedicine, J Control Release, 146 (2010) 2-5.

[15] W.Y. Huang, J.J. Davis, Multimodality and nanoparticles in medical imaging, Dalton Trans, 40 (2011) 6087-6103.

[16] T. Minko, L. Rodriguez-Rodriguez, V. Pozharov, Nanotechnology approaches for personalized treatment of multidrug resistant cancers, Adv Drug Deliv Rev, 65 (2013) 1880-1895.

[17] L.L. Wang, J.A. Burdick, Engineered Hydrogels for Local and Sustained Delivery of RNA-Interference Therapies, Adv Healthc Mater, 6 (2017).

[18] M.F. Attia, N. Anton, J. Wallyn, Z. Omran, T.F. Vandamme, An overview of active and passive targeting strategies to improve the nanocarriers efficiency to tumour sites, J Pharm Pharmacol, (2019).

[19] A. George, P.A. Shah, P.S. Shrivastav, Natural biodegradable polymers based nano-formulations for drug delivery: A review, Int J Pharm, 561 (2019) 244-264.

[20] R. Savla, O.B. Garbuzenko, S. Chen, L. Rodriguez-Rodriguez, T. Minko, Tumor-targeted responsive nanoparticle-based systems for magnetic resonance imaging and therapy, Pharm Res, 31 (2014) 3487-3502.

[21] P. Chandna, J.J. Khandare, E. Ber, L. Rodriguez-Rodriguez, T. Minko, Multifunctional tumor-targeted polymer-peptide-drug delivery system for treatment of primary and metastatic cancers, Pharm Res, 27 (2010) 2296-2306.

[22] P. Chandna, M. Saad, Y. Wang, E. Ber, J. Khandare, A. Vetcher, V. Soldatenkov, T. Minko, Targeted proapoptotic anticancer drug delivery system, Molecular Pharmaceutics, 5 (2007) 668-678.

[23] T. Minko, R. Pakunlu, Y. Wang, J. Khandare, M. Saad, New Generation of Liposomal Drugs for Cancer, Anti-Cancer Agents in Medicinal Chemistry, 6 (2006) 537-552.

[24] S.S. Dharap, P. Chandna, Y. Wang, J.J. Khandare, B. Qiu, S. Stein, T. Minko, Molecular targeting of BCL2 and BCLXL proteins by synthetic BCL2 homology 3 domain peptide enhances the efficacy of chemotherapy, J Pharmacol Exp Ther, 316 (2006) 992-998.

[25] M. Devouassoux-Shisheboran, C. Genestie, Pathobiology of ovarian carcinomas, Chin J Cancer, 34 (2015) 50-55.

[26] E.A. Eisenhauer, Real-world evidence in the treatment of ovarian cancer, Ann Oncol, 28 (2017) viii61-viii65.

[27] L.A. Torre, B. Trabert, C.E. DeSantis, K.D. Miller, G. Samimi, C.D. Runowicz, M.M. Gaudet, A. Jemal, R.L. Siegel, Ovarian cancer statistics, 2018, CA Cancer J Clin, 68 (2018) 284-296.

[28] C. Rooth, Ovarian cancer: risk factors, treatment and management, British Journal of Nursing, 25 (2013) S23-30.

[29] C. Cardenas, A.B. Alvero, B.S. Yun, G. Mor, Redefining the origin and evolution of ovarian cancer: a hormonal connection, Endocr Relat Cancer, 23 (2016) R411-422.

[30] A.C. Society, Ovarian Cancer Stages, Early Detection, Diagnosis, and Staging 2018.

[31] C.T.C.o. America, Ovarian cancer stages, (2019).

[32] S. Javadi, D.M. Ganeshan, A. Qayyum, R.B. Iyer, P. Bhosale, Ovarian Cancer, the Revised FIGO Staging System, and the Role of Imaging, AJR Am J Roentgenol, 206 (2016) 1351-1360.

[33] M.H. Ebell, M.B. Culp, T.J. Radke, A Systematic Review of Symptoms for the Diagnosis of Ovarian Cancer, Am J Prev Med, 50 (2016) 384-394.

[34] S. Sundar, R.D. Neal, S. Kehoe, Diagnosis of ovarian cancer, BMJ, 351 (2015) h4443.

[35] U.A. Matulonis, A.M. Oza, T.W. Ho, J.A. Ledermann, Intermediate clinical endpoints: a bridge between progression-free survival and overall survival in ovarian cancer trials, Cancer, 121 (2015) 1737-1746.

[36] F. Guffanti, R. Fruscio, E. Rulli, G. Damia, The impact of DNA damage response gene polymorphisms on therapeutic outcomes in late stage ovarian cancer, Sci Rep, 6 (2016) 38142.

[37] E. Stoeckle, L. Bourdarias, F. Guyon, S. Croce, V. Brouste, L. Thomas, A. Floquet, Progress in survival outcomes in patients with advanced ovarian cancer treated by neo-adjuvant platinum/taxane-based chemotherapy and late interval debulking surgery, Ann Surg Oncol, 21 (2014) 629-636.

[38] A.P. Makar, C.G. Trope, P. Tummers, H. Denys, K. Vandecasteele, Advanced Ovarian Cancer: Primary or Interval Debulking? Five Categories of Patients in View of the Results of Randomized Trials and Tumor Biology: Primary Debulking Surgery and Interval Debulking Surgery for Advanced Ovarian Cancer, Oncologist, 21 (2016) 745-754.

[39] S. Tangjitgamol, S. Manusirivithaya, M. Laopaiboon, P. Lumbiganon, A. Bryant, Interval debulking surgery for advanced epithelial ovarian cancer, Cochrane Database Syst Rev, (2016) CD006014.

[40] H. Azais, J.P. Estevez, P. Foucher, Y. Kerbage, S. Mordon, P. Collinet, Dealing with microscopic peritoneal metastases of epithelial ovarian cancer. A surgical challenge, Surg Oncol, 26 (2017) 46-52.

[41] L. Norouzi-Barough, M.R. Sarookhani, M. Sharifi, S. Moghbelinejad, S. Jangjoo, R. Salehi, Molecular mechanisms of drug resistance in ovarian cancer, J Cell Physiol, 233 (2018) 4546-4562.

[42] E.L. Christie, D.D.L. Bowtell, Acquired chemotherapy resistance in ovarian cancer, Ann Oncol, 28 (2017) viii13-viii15.

[43] X. Liu, Y. Gao, Y. Lu, J. Zhang, L. Li, F. Yin, Oncogenes associated with drug resistance in ovarian cancer, J Cancer Res Clin Oncol, 141 (2015) 381-395.

[44] A.E. Freimund, J.A. Beach, E.L. Christie, D.D.L. Bowtell, Mechanisms of Drug Resistance in High-Grade Serous Ovarian Cancer, Hematol Oncol Clin North Am, 32 (2018) 983-996.

[45] PubChem, Doxorubicin, Compound Summary, U.S National Library of Medicine, 2019.

[46] K.M. Pos, Drug transport mechanism of the AcrB efflux pump, Biochim Biophys Acta, 1794 (2009) 782-793.

[47] J. Au, S. Jang, C. Chen, L. Song, L. Hu, M. Wientjes, Determinants of drug delivery and transport to solid tumors, Journal of Controlled Release, 74 (2001) 31-46.

[48] L.B. Liao, H.Y. Zhou, X.M. Xiao, Spectroscopic and viscosity study of doxorubicin interaction with DNA, Journal of Molecular Structure, 749 (2005) 108-113.

[49] F. Fornari, J. Randolph, J. Yalowich, M. Ritke, D. Genwirtz, Interference by doxorubicin with DNA unwinding in MCF-7 breast tumor cells, Molecular Pharmacology, 45 (1994) 649-656.

[50] K. Hande, Clinical applications of anticancer drugs targeted to topoisomerase II, Biochimica et Biophysica Acta, 1400 (1998) 173-184.

[51] R. Momparler, M. Karon, S. Siegel, F. Avila, Effect of adriamycin on DNA, RNA, and protein synthesis in cell-free systems and intact cells, Cancer Research, 36 (1976) 2891-2895.

[52] X. Yang, A. Wang, Structural studies of atom-specific anticancer drugs acting on DNA, Pharmacology and Therapeutics, 83 (1999) 181-215.

[53] N.C. Institute, Doxorubicin Hydrochloride, in: N.C. Institute (Ed.) Cancer Treatment, 2018.

[54] S. Rossi, Australian Medicines Handbook, 2013 ed., Adelaide2013.

[55] E. Ravina, Drugs from Microbiological Sources, The evolution of Drug Discovery: From Traditional Medicines to Modern Drugs, Wiley & Sons, pp. 291-292.

[56] Chemocare, Doxorubicin, Drug Info, 2019.

[57] S. Pignata, C.C. S, A. Du Bois, P. Harter, F. Heitz, Treatment of recurrent ovarian cancer, Ann Oncol, 28 (2017) viii51-viii56.

[58] Y. Barenholz, Doxil(R)--the first FDA-approved nano-drug: lessons learned, J Control Release, 160 (2012) 117-134.

[59] M. Wani, H. Taylor, M. Wall, P. Coggon, A. McPhail, Plant antitumor agents. VI. The isolation and structure of taxol, a novel antileukemic and antitumor agent from Taxus brevifolia, Journal of the American Chemical Society, 93 (1971) 2325-2327.

[60] M. Caruso, A. Colombo, N. Crespi-Perellino, L. Fedeli, J. Malyszko, A. Pavesi, S. Quaroni, M. Saracchi, G. Ventrella, Studies on a strain of paclitaxel producer, Annals of Microbiology, 50 (2000) 89-102.

[61] A. Stierle, G. Strobel, D. Stierle, Taxol and taxane production by Taxomyces andreanae, an endophytic fungus of Pacific yew, Science, 260 (1993) 214-216.

[62] W. Stull, T. Scales, Taxol®(Paclitaxel), Applied Biochemistry and Biotechnology, 54 (1995) 133-140.

[63] K. Downing, Structural basis for the interaction of tubulin with proteins and drugs that affect microtubule dynamics, Annual Review of Cell and Developmental Biology, 16 (2000) 89-111.

[64] A. Jordan, J. Hadfield, N. Lawrence, A. McGown, Tubulin as a target for anticancer drugs: agents which interact with the mitotic spindle, Medicinal Research Reviews, 18 (1998) 259-296.

[65] S. Horwitz, Taxol (paclitaxel): mechanisms of action, Annal of Oncology, 5 (1994) S3-6.

[66] W. McGuire, W. Hoskins, M. Brady, P. Kucera, E. Partridge, K. Look, D. Clarke-Pearson, M. Davidson, Cyclophosphamide and cisplatin compared with

paclitaxel and cisplatin in patients with stage III and stage IV ovarian cancer, The New England Jounral of Medicine, 334 (1996) 1-6.

[67] M. Piccart, K. Bertelsen, K. James, J. Cassidy, C. Mangioni, E. Simonsen, G. Stuart, S. Kaye, I. Vergote, R. Blom, R. Grimshaw, R. Atkinson, K. Swenerton, C. Trope, M. Nardi, J. Kaern, S. Tumolo, P. Timmers, J. Roy, F. Lhoas, B. Lindvall, M. Bacon, A. Birt, J. Andersen, B. Zee, J. Paul, B. Baron, S. Pecorelli, Randomized intergroup trial of cisplatin-paclitaxel versus cisplatin-cyclophosphamide in women with advanced epithelial ovarian cancer: three-year results, Journal of the National Cancer Institution, 92 (2000) 699-708.

[68] C. Marth, D. Reimer, A.G. Zeimet, Front-line therapy of advanced epithelial ovarian cancer: standard treatment, Ann Oncol, 28 (2017) viii36-viii39.

[69] M.X. Lee, D.S. Tan, Weekly versus 3-weekly paclitaxel in combination with carboplatin in advanced ovarian cancer: which is the optimal adjuvant chemotherapy regimen?, J Gynecol Oncol, 29 (2018) e96.

[70] R. Ozols, Paclitaxel (Taxol)/carboplatin combination chemotherapy in the treatment of advanced ovarian cancer, Seminars in Oncology, 27 (2000) 3-7.

[71] M.A. Bookman, Optimal primary therapy of ovarian cancer, Ann Oncol, 27 Suppl 1 (2016) i58-i62.

[72] A. Singla, A. Garg, D. Aggarwal, Paclitaxel and its formulations, International Journal of Pharmaceutics, 235 (2002) 179-192.

[73] S. Kumar, H. Mahdi, C. Bryant, J.P. Shah, G. Garg, A. Munkarah, Clinical trials and progress with paclitaxel in ovarian cancer, Int J Womens Health, 2 (2010) 411-427.

[74] H. Gelderblom, J. Verweij, K. Nooter, A. Sparreboom, Cremophor EL - the drawbacks and advantages of vehicle selection for drug formulation, European Journal of Cancer, 37 (2001) 1590-1598.

[75] M.N. Kundranda, J. Niu, Albumin-bound paclitaxel in solid tumors: clinical development and future directions, Drug Des Devel Ther, 9 (2015) 3767-3777.

[76] D.A. Yardley, nab-Paclitaxel mechanisms of action and delivery, J Control Release, 170 (2013) 365-372.

[77] A.R. de Biasi, J. Villena-Vargas, P.S. Adusumilli, Cisplatin-induced antitumor immunomodulation: a review of preclinical and clinical evidence, Clin Cancer Res, 20 (2014) 5384-5391.

[78] D. Lebwohl, R. Canetta, Clinical development of platinum complexes in cancer therapy: an historical perspective and an update, European Journal of Cancer, 34 (1998) 1522-1534.

[79] B. Rosenberg, L. VanCamp, J. Trosko, V. Mansour, Platinum compounds: a new class of potent antitumour agents, Nature, 222 (1969) 385-386.

[80] B. Rosenberg, L. VanCamp, The successful regression of large solid sarcoma 180 tumors by platinum compounds, Cancer Research, 30 (1970) 1799-1802.

[81] D. Carpenter, Reputation and Power: Organizational Image and Pharmaceutical Regulation at the FDA, Princton University Press2010.

[82] Y.P. Ho, S.C. Au-Yeung, K.K. To, Platinum-based anticancer agents: innovative design strategies and biological perspectives, Med Res Rev, 23 (2003) 633-655.

[83] Z. Yue, Z. Cao, Current Strategy for Cisplatin Delivery, Current Cancer Drug Targets, 116 (2016) 480-488.

[84] S. Dasari, P.B. Tchounwou, Cisplatin in cancer therapy: molecular mechanisms of action, Eur J Pharmacol, 740 (2014) 364-378.

[85] T. Boulikas, M. Vougiouka, Cisplatin and platinum drugs at the molecular level, Oncology Reports, 10 (2003) 1663-1682.

[86] S. Cohen, S. Lippard, Cisplatin: from DNA damage to cancer chemotherapy, Progress in Nucleic Acid Research and Molecular Biology, 67 (2001) 93-130.

[87] L. Kellard, S. Sharp, C. O'Neill, F. Raynaud, P. Beale, I. Judson, Mini-review: discovery and development of platinum complexes designed to circumvent cisplatin resistance, Jounral of Inorganic Biochemistry, 77 (1999) 111-115.

[88] B. Stordal, M. Davey, Understanding cisplatin resistance using cellular models, IUBMB Life, 59 (2007) 696-699.

[89] L. Kellard, C. Barnard, K. Mellish, M. Jones, P. Goddard, M. Valenti, A. Bryant, B. Murrer, K. Harrap, A novel trans-platinum coordination complex possessing in vitro and in vivo antitumor activity, Cancer Research, 54 (1994) 5618-5622.

[90] P. Mistry, L. Kelland, G. Abel, S. Sidhar, K. Harrap, The relationships between glutathione, glutathione-S-transferase and cytotoxicity of platinum drugs and melphalan in eight human ovarian carcinoma cell lines, British Journal of Cancer, 64 (1991) 215-220.

[91] G.P. Stathopoulos, Liposomal cisplatin: a new cisplatin formulation, Anticancer Drugs, 21 (2010) 732-736.

[92] K. Loeb, Significance of Multiple Mutations in Cancer, Carcinogenesis, 21 (2000) 379-385.

[93] C. Ricciardelli, M.K. Oehler, Diverse molecular pathways in ovarian cancer and their clinical significance, Maturitas, 62 (2009) 270-275.

[94] R. Kurman, I. Shih, The Origin and Pathogenesis of Epithelial Ovarian Cancer:A Proposed Unifying Theory, American Journal of Surgical Pathology, 34 (2010) 433-443.

[95] M. Monaco, Fatty acid metabolism in breast cancer subtypes, Oncotarget, 8 (2017) 29487-29500.

[96] E. Fessler, J.P. Medema, Colorectal Cancer Subtypes: Developmental Origin and Microenvironmental Regulation, Trends Cancer, 2 (2016) 505-518.

[97] Y. Zhang, D.C. Wang, L. Shi, B. Zhu, Z. Min, J. Jin, Genome analyses identify the genetic modification of lung cancer subtypes, Semin Cancer Biol, 42 (2017) 20-30.

[98] M. Kossi, A. Leary, J. Scoazec, C. Genestie, Ovarian Cancer: A Heterogeneous Disease, Pathobiology, 85 (2018) 41-49.

[99] X. Yue, Y. Zhao, Y. Xu, M. Zheng, Z. Feng, W. Hu, Mutant p53 in Cancer: Accumulation, Gain-of-Function, and Therapy, J Mol Biol, 429 (2017) 1595-1606.

[100] K.M. Zbuk, C. Eng, Cancer phenomics: RET and PTEN as illustrative models, Nat Rev Cancer, 7 (2007) 35-45.

[101] M. Jasin, Homologous repair of DNA damage and tumorigenesis: the BRCA connection, Oncogene, 21 (2002) 8981-8993.

[102] P. Chouvardas, G. Kollias, C. Nikolaou, Inferring active regulatory networks from gene expression data using a combination of prior knowledge and enrichment analysis, BMC Bioinformatics, 17 Suppl 5 (2016) 181.

[103] J. Crocker, G.R. Ilsley, Using synthetic biology to study gene regulatory evolution, Curr Opin Genet Dev, 47 (2017) 91-101.

[104] T.M. Kim, P.J. Park, Advances in analysis of transcriptional regulatory networks, Wiley Interdiscip Rev Syst Biol Med, 3 (2011) 21-35.

[105] A. Molchadsky, V. Rotter, p53 and its mutants on the slippery road from stemness to carcinogenesis, Carcinogenesis, 38 (2017) 347-358.

[106] F. Chen, X. Zhuang, L. Lin, P. Yu, Y. Wang, Y. Shi, G. Hu, Y. Sun, New horizons in tumor microenvironment biology: challenges and opportunities, BMC Med, 13 (2015) 45.

[107] W. Du, O. Elemento, Cancer systems biology: embracing complexity to develop better anticancer therapeutic strategies, Oncogene, 34 (2015) 3215-3225.

[108] P.K. Kreeger, D.A. Lauffenburger, Cancer systems biology: a network modeling perspective, Carcinogenesis, 31 (2010) 2-8.

[109] E. Liu, D.A. Lauffenburger, Systems Biomedicine: Concepts and Perspectives, Elsevier Science2009.

[110] E. Barillot, L. Calzone, P. Hupe, J. Vert, A. Zinovyev, Computational Systems Biology of Cancer, Taylor & Francis2012.

[111] S. Manier, K. Salem, J. Park, D. Landau, G. Getz, I. Ghobrial, Genomic complexity of multiple myeloma and its clinical implications, Nature Reviews Clinical Oncology, 14 (2017) 100-113.

[112] J. Maciejewski, S. Balasubramanian, Clinical implications of somatic mutations in aplastic anemia and myelodysplastic syndrome in genomic age, Hematology American Society of Hematological Education Program, 17 (2017) 66-72.

[113] A.N. Abou Tayoun, B. Krock, N.B. Spinner, Sequencing-based diagnostics for pediatric genetic diseases: progress and potential, Expert Rev Mol Diagn, 16 (2016) 987-999.

[114] R.L. Haspel, R.J. Olsen, A. Berry, C.E. Hill, J.D. Pfeifer, I. Schrijver, K.L. Kaul, Progress and potential: training in genomic pathology, Arch Pathol Lab Med, 138 (2014) 498-504.

[115] R. Moshehi, W. Chu, D. Kalan, D. Fishman, H. Risch, A. Fields, D. Smotkin, Y. Ben-David, D. Reosenblatt, D. Russo, P. Schwartz, N. Tung, E. Waner, B. Rosen, J. Friedman, J. Brunet, S. Narod, BRCA1 and BRCA2 Mutation Analysis of 208 Ashkenazi Jewish Women, The American Society of Human Genetics, 66 (2000) 1272-2000.

[116] A. Whitemore, G. Gong, J. Itnye, Prevalence and Contribution of BRCA1 Mutations in Breast Cancer and Ovarian Cancer: Results from Three US Population=Based Case-Control Sudies of Ovarian Cancer, The American Society of Human Genetics, 60 (1997) 496-504.

[117] H. Risch, J. McLaughlin, D. Cole, B. Rosen, L. Bradley, E. Kwan, E. Jack, D. Vesprini, G. Kuperstein, J. Abrahamson, Prevalence and Penetrance of Germline BRCA1 and BRCA2 Mutations in a Population of 649 women with Ovarian Cancer, The American Society of Human Genetics, 68 (2001) 700-710.

[118] G. Encinas, S. Maistro, F.S. Pasini, M.L. Katayama, M.M. Brentani, G.H. Bock, M.A. Folgueira, Somatic mutations in breast and serous ovarian cancer

young patients: a systematic review and meta-analysis, Rev Assoc Med Bras (1992), 61 (2015) 474-483.

[119] B. Gold, Somatic mutations in cancer: Stochastic versus predictable, Mutat Res, 814 (2017) 37-46.

[120] E. Despierre, D. Lambrechts, P. Neven, F. Amant, S. Lambrechts, I. Vergote, The molecular genetic basis of ovarian cancer and its roadmap towards a better treatment, Gynecol Oncol, 117 (2010) 358-365.

[121] D.R. Rhodes, A.M. Chinnaiyan, Integrative analysis of the cancer transcriptome, Nat Genet, 37 Suppl (2005) S31-37.

[122] A. Stahlberg, N. Zoric, P. Aman, M. Kubista, Quantitative real-time PCR for cancer detection: the lymphoma case, Expert Review of Molecular Diagnostics, 5 (2005) 221-230.

[123] J. Aerts, W. Wynendaele, R. Paridaens, M. Christiaens, W. Van Der Bogaert, A. Van Oosterom, F. Vandekerckhove, A real-time quantitative reverse transcriptase polymerase chain reaction (RT-PCR) to detect breast cancer, Annual Oncology, 12 (2001) 39-49.

[124] S. Warrenfeltz, S. Pavlik, S. Datta, E.T. Kraemer, B. Benigno, J.F. McDonald, Gene expression profiling of epithelial ovarian tumours correlated with malignant potential, Mol Cancer, 3 (2004) 27.

[125] M. Van Der Vijver, Y. He, L. Van't Veer, H. Dai, A. Hart, D. Voskuil, G. Schreiber, J. Peterse, C. Roberts, M. Marton, M. Parrish, D. Atsma, A. Witteveen, A. Glas, L. Delahaye, T. Van Der Velde, H. Bartelink, S. Rodenhuis, E. Rutgers, S. Friend, R. Bernards, A Gene Expression Signature as a Predictor of Survival in Breast Cancer, The New England Jounral of Medicine, 339 (2002) 1999-2009.

[126] M. Arya, I. Shergill, M. Williamson, L. Gommersall, N. Arya, H. Patel, Basic principles of real-time quantitative PCR, Expert Review of Molecular Diagnostics, 2 (2014) 209-219.

[127] M. Marzancola, A. Sedighi, P. Li, DNA Microarray-Based Diagnostics, Humana Press, New York, NY, 2016.

[128] R. Bianco, T. Gelardi, V. Damiano, F. Ciardiello, G. Tortora, Rational bases for the development of EGFR inhibitors for cancer treatment, Int J Biochem Cell Biol, 39 (2007) 1416-1431.

[129] D.R. Khan, M.N. Webb, T.H. Cadotte, M.N. Gavette, Use of Targeted Liposome-based Chemotherapeutics to Treat Breast Cancer, Breast Cancer (Auckl), 9 (2015) 1-5.

[130] C.P. Leamon, J.A. Reddy, Folate-targeted chemotherapy, Adv Drug Deliv Rev, 56 (2004) 1127-1141.

[131] I.R. Vlahov, H.K. Santhapuram, P.J. Kleindl, S.J. Howard, K.M. Stanford, C.P. Leamon, Design and regioselective synthesis of a new generation of targeted chemotherapeutics. Part 1: EC145, a folic acid conjugate of desacetylvinblastine monohydrazide, Bioorg Med Chem Lett, 16 (2006) 5093-5096.

[132] R.W. Naumann, R.L. Coleman, R.A. Burger, E.A. Sausville, E. Kutarska, S.A. Ghamande, N.Y. Gabrail, S.E. Depasquale, E. Nowara, L. Gilbert, R.H. Gersh, M.G. Teneriello, W.A. Harb, P.A. Konstantinopoulos, R.T. Penson, J.T. Symanowski, C.D. Lovejoy, C.P. Leamon, D.E. Morgenstern, R.A. Messmann, PRECEDENT: a randomized phase II trial comparing vintafolide (EC145) and pegylated liposomal doxorubicin (PLD) in combination versus PLD alone in patients with platinum-resistant ovarian cancer, J Clin Oncol, 31 (2013) 4400-4406.

[133] B.C. Schmid, M.K. Oehler, New perspectives in ovarian cancer treatment, Maturitas, 77 (2014) 128-136.

[134] C. Grundker, A. Gunthert, S. Westphalen, G. Emons, Biology of the gonadotropin-releasing hormone system in gynecological cancers, European Journal of Endocrinology, 146 (2002) 1-14.

[135] C. Gründker, P. Völker, F. Griesinger, A. Ramaswamy, A. Nagy, A.V. Schally, G. Emons, Antitumor effects of the cytotoxic luteinizing hormone–releasing hormone analog AN-152 on human endometrial and ovarian cancers xenografted into nude mice, American Journal of Obstetrics and Gynecology, 187 (2002) 528-537.

[136] S.S. Dharap, T. Minko, Targeted proapoptotic LHRH-BH3 peptide, Pharmaceutical Research, 20 (2003) 889-896.

[137] T. Minko, M. Patil, M. Zhang, J. Khandare, M. Saad, P. Chandna, O. Taratula, LHRH-Targeted Nanoparticles for Cancer Therapeutics, Methods of Molecular Biology, 624 (2010) 281-294.

[138] M. Gottesman, Mechanisms of Cancer Drug Resistance, Annunal Reveiw of Medicine, 53 (2002) 615-627.

[139] R. Cornelison, D.C. Llaneza, C.N. Landen, Emerging Therapeutics to Overcome Chemoresistance in Epithelial Ovarian Cancer: A Mini-Review, Int J Mol Sci, 18 (2017).

[140] G. Emons, H. Sindermann, J. Engel, A.V. Schally, C. Grundker, Luteinizing hormone-releasing hormone receptor-targeted chemotherapy using AN-152, Neuroendocrinology, 90 (2009) 15-18.

[141] M. Zhang, O.B. Garbuzenko, K. Rehul, L. Rodriguez-Rodriguez, T. Minko, Two-in-one: combined targeted chemo and gene therapy for tumor suppression and prevention of metastases, Nanomedicine (Lond), 7 (2012) 185-197.

[142] M. Mogler, K. Kamrud, RNA-based viral vectors, Expert Review of Vaccines, 14 (2014) 283-312.

[143] K.A. White, L. Enjuanes, B. Berkhout, RNA virus replication, transcription and recombination, RNA Biol, 8 (2011) 182-183.

[144] E. Bernstein, A. Caudy, S. Hammond, G. Hannon, Role for a bidentate ribonuclease in the initiation step of RNA interference, Nature, 409 (2001) 363-666.

[145] C. Matranga, Y. Tomari, C. Shin, D.P. Bartel, P.D. Zamore, Passenger-strand cleavage facilitates assembly of siRNA into Ago2-containing RNAi enzyme complexes, Cell, 123 (2005) 607-620.

[146] S. Hammond, E. Bernstein, D. Beach, G. Hannon, An RNA-directed nuclease mediates post-transcriptional gene silencing in Drosophila cells, Nature, 404 (2000) 293-296.

[147] G. Hutvagner, P.D. Zamore, A microRNA in a multiple-turnover RNAi enzyme complex, Science, 297 (2002) 2056-2060.

[148] A. Fire, S. Xu, M. Montgomery, S. Kostas, S. Driver, C. Mello, Potent and specific genetic interference by double-stranded RNA in Caenorhabditis elegans, Nature, 391 (1998) 806-811.

[149] J. Kennerdell, R. Carthew, Use of dsRNA-mediated genetic interference to demonstrate that frizzled and frizzled 2 act in the wingless pathway, Cell, 95 (1998) 1017-1026.

[150] H. Ngo, C. Tschudi, K. Gull, E. Ullu, Double-stranded RNA induces mRNA degradation in Trypanosoma brucei, Proceedings of the National Academy of Science of the USA, 95 (1998) 14687-14692.

[151] A. Sanchez Alvarado, P. Newmark, Double-stranded RNA specifically disrupts gene expression during planarian regeneration, Proceedings of the National Academy of Science of the USA, 96 (1999) 5049-5054.

[152] J. Lohmann, I. Endl, T. Bosch, Silencing of developmental genes in Hydra, Developmental Biology, 214 (1999) 211-214.

[153] A. Hamilton, D. Baulcombe, A species of small antisense RNA in posttranscriptional gene silencing in plants, Science, 286 (1999) 950-952.

[154] S. Elbashir, J. Harborth, W. Lendeckel, A. Yaicin, K. Weber, T. Tuschi, Duplexes of 21-nucleotide RNAs mediate RNA interference in cultured mammalian cells, Nature, 411 (2001) 494-498.

[155] T. Tuschil, RNA interference and small interfering RNAs, Chembiochem, 2 (2001) 239-245.

[156] M.L. Patil, M. Zhang, S. Betigeri, O. Taratula, H. He, T. Minko, Surface-modified and internally cationic polyamidoamine dendrimers for efficient siRNA delivery, Bioconjug Chem, 19 (2008) 1396-1403.

[157] M.L. Patil, M. Zhang, T. Minko, Multifunctional Triblock Nanocarrier (PAMAM-PEG-PLL) for the Efficient Intracellular siRNA Delivery and Gene Silencing, American Chemical Society Nano, 5 (2011) 1877-1887.

[158] Y. Higuchi, S. Kawakami, M. Hashida, Strategies for in vivo delivery of siRNAs: recent progress, BioDrugs, 24 (2010) 195-205.

[159] M. Morpurgo, C. Monfardini, L. Hofland, M. Sergi, P. Orsolini, J. Dumont, F. Veronese, Selective alkylation and acylation of alpha and epsilon amino groups with PEG in a somatostatin analogue: tailored chemistry for optimized bioconjugates, Bioconjugugate Chemistry, 13 (2002) 1238-1243.

[160] K. Park, Controlled drug delivery systems: past forward and future back, J Control Release, 190 (2014) 3-8.

[161] N. Maurer, D. Fenske, P. Cullis, Developments in liposomal drug delivery systems, Expert Opin Biol Ther, 1 (2001) 923-947.

[162] P. Pattnaik, T. Ray, Improving liposome integrity and easing bottlenecks to production, Pharm Tech Euro, 22 (2009).

[163] A. Chonn, P. Cullis, Recent advances in liposomal drug-delivery systems, Curr Opin Biotechnol, 6 (1995) 698-708.

[164] A. Samad, Y. Sultana, M. Agil, Liposomal drug delivery systems: an update review, Curr Drug Deliv, 4 (2007) 297-305.

[165] A. Bangham, Development of the Liposome Concept, Liposomes in Biological Systems, John Wiley & Sons1980, pp. 1-24.

[166] A. Wagner, K. Vorauer-Uhl, Liposome Technology for Industrial Purposes, J Drug Deliv, 2011 (2011) 9.

[167] C.G. Siontorou, G.P. Nikoleli, D.P. Nikolelis, S.K. Karapetis, Artificial Lipid Membranes: Past, Present, and Future, Membranes (Basel), 7 (2017).

[168] P. Goyal, K. Goyal, S. Vijaya Kumar, A. Singh, O. Katare, D. Mishra, Liposomal drug delivery systems--clinical applications, Acta Pharm, 55 (2005) 1-25.

[169] R. Hofheinz, S. Gnad-Vogt, U. Beyer, A. Hochhaus, Liposomal encapsulated anti-cancer drugs, Anticancer Drugs, 16 (2005) 691-707.

[170] G. Sessa, G. Weissmann, Incorporation of Lysozyme into Liposomes: A model for Structure-Linked Latency, J Biol Chem, 245 (1970) 3295-3301.

[171] G. Gregoriadis, Enzyme Entrapment in Liposomes, Methods Enzymol, 44 (1976) 218-227.

[172] R. Schwendener, H. Schott, Liposome formulations of hydrophobic drugs, Methods Mol Bio, 605 (2010) 129-138.

[173] V. Joguparthi, T.X. Xiang, B.D. Anderson, Liposome transport of hydrophobic drugs: gel phase lipid bilayer permeability and partitioning of the lactone form of a hydrophobic camptothecin, DB-67, J Pharm Sci, 97 (2008) 400-420.

[174] R. Gennis, Interactions of Small Molecules with Membranes: Partitioning, Permeability, and Electrical Effects, Biomembranes, Springer, New York, NY, 1989, pp. 235-269.

[175] F. Roerdink, N. Wassef, E. Richardson, C. Alving, Effects of negatively charged lipids on phagocytosis of liposomes opsonized by complement, Biochim Biophys Acta, 734 (1983) 33-39.

[176] J. Li, X. Wang, T. Zhang, C. Wang, Z. Huang, X. Luo, Y. Deng, A review on phospholipids and their main applications in drug delivery systems, Asian Journal of Pharmaceutical Sciences, 10 (2015) 81-98.

[177] A. Schroeder, C.G. Levins, C. Cortez, R. Langer, D.G. Anderson, Lipid-based nanotherapeutics for siRNA delivery, J Intern Med, 267 (2010) 9-21.

[178] P. Campbell, Toxicity of some charged lipids used in liposome preparations, Cytobios, 37 (1983) 21-26.

[179] L. Sercombe, T. Veerati, F. Moheimani, S.Y. Wu, A.K. Sood, S. Hua, Advances and Challenges of Liposome Assisted Drug Delivery, Frontiers in Pharmacology, 6 (2015).

[180] A. Gabizon, D. Papahadjopoulos, The role of surface charge and hydrophilic groups on liposome clearance in vivo, Biochim Biophys Acta, 1103 (1992) 94-100.

[181] P. Cullis, A. Chonn, S. Semple, Interactions of liposomes and lipid-based carrier systems with blood proteins: Relation to clearance behaviour in vivo, Adv Drug Deliv Rev, 32 (1998) 3-17.

[182] N. Oku, Y. Namba, S. Okada, Tumor accumulation of novel RES-avoiding liposomes, Biochim Biophys Acta, 1126 (1992) 255-260.

[183] T. Allen, C. Hansen, F. Martin, C. Redemann, A. Yau-Young, Liposomes containing synthetic lipid derivatives of poly(ethylene glycol) show prolonged circulation half-lives in vivo, Biochim Biophys Acta, 1066 (1991) 29-36.

[184] M. Webb, T. Harasym, D. Masin, M. Bally, L. Mayer, Sphingomyelin-cholesterol liposomes significantly enhance the pharmacokinetic and therapeutic properties of vincristine in murine and human tumour models, Br J Cancer, 72 (1995) 896-904.

[185] P. Yingchoncharoen, D.S. Kalinowski, D.R. Richardson, Lipid-Based Drug Delivery Systems in Cancer Therapy: What Is Available and What Is Yet to Come, Pharmacol Rev, 68 (2016) 701-787.

[186] G. Bozzuto, A. Molinari, Liposomes as nanomedical devices, Int J Nanomedicine, 10 (2015) 975-999.

[187] B. Klajnert, M. Bryszewska, Dendrimers: properties and applications, Acta Biochem Pol, 48 (2001) 199-208.

[188] J. Frechet, Functional polymers and dendrimers: reactivity, molecular architecture, and interfacial energy, Science, 263 (1994) 1710-1715.

[189] A. Archut, F. Vogtle, Functional cascade molecules, Chem Soc Rev, 27 (1998).

[190] Y. Cheng, Z. Xu, M. Ma, T. Xu, Dendrimers as drug carriers: applications in different routes of drug administration, J Pharm Sci, 97 (2008) 123-143.

[191] T. Sakthivel, Adsorption of amphipathic dendrons on polystyrene nanoparticles, International Journal of Pharmaceutics, 254 (2003) 23-26.

[192] E. Buhleirer, W. Wehner, F. Vogtle, "Cascade"- and "Nonskid-Chain-like" Syntheses of Molecular Cavity Topologies, Synthesis, 1978 (1978) 155-158.

[193] D. Tomalia, A. Naylor, W. Goddard, Starburst Dendrimers: Molecular-Level Control of Size, Shape, Surface Chemistry, Topology, and Flexibility from Atoms to Macroscopic Matter, Angew Chem Int Ed, 29 (1990) 139-175.

[194] F. Tack, A. Bakker, S. Maes, N. Dekeyser, M. Bruining, C. Elissen-Roman, M. Janicot, M. Brewster, H. Janssen, B. De Waal, P. Fransen, X. Lou, E. Meijer,

Modified poly(propylene imine) dendrimers as effective transfection agents for catalytic DNA enzymes (DNAzymes), J Drug Target, 14 (2006) 69-86.

[195] N. Jain, A. Khopade, Dendrimers as Potential Delivery Systems for Bioactives, Advances in controlled and novel drug delivery, CBS2001.

[196] S.M. Grayson, J.M.J. Fréchet, Convergent Dendrons and Dendrimers: from Synthesis to Applications, Chemical Reviews, 101 (2001) 3819-3868.

[197] B. Hari, K. Kalamagal, R. Porkodi, P. Gajula, J. Ajay, Dendrimer: Globular Nanostructured Materials for Drug Delivery, International Journal of PharmTech Research, 4 (2012) 432-451.

[198] E. Van Den Berg, E. Meijer, Poly(propylene imine) Dendrimers: Large:-Scale Synthesis by Hetereogeneously Catalyzed Hydrogenations, Angew Chem Int Ed, 32 (1993) 1308-1311.

[199] A. Chen, L. Sandthakumaran, S. Nair, P. Amenta, T. Thomas, H. He, T. Thomas, Oligodeoxynucleotide nanostructure formation in the presence of polypropyleneimine dendrimers and their uptake in breast cancer cells, Nanotechnology, 17 (2006) 5449-5460.

[200] A. Hollins, M. Benboubetra, B. Zinselmeyer, A. Schatzlein, I. Uchegbu, S. Akhtar, Evaluation of generation 2 and 3 poly(propylenimine) dendrimers for the potential cellular delivery of antisense oligonucleotides targeting the epidermal growth factor receptor, Pharm Res, 21 (2004) 458-466.

[201] A.G. Schatzlein, B.H. Zinselmeyer, A. Elouzi, C. Dufes, Y.T. Chim, C.J. Roberts, M.C. Davies, A. Munro, A.I. Gray, I.F. Uchegbu, Preferential liver gene expression with polypropylenimine dendrimers, J Control Release, 101 (2005) 247-258.

[202] SeleXel, RNA interference, Technology and Productshttp://selexel.com/en/science-2-2/rna-interference/, 2016.

[203] C. Costa, J.-M. Costa, C. Desterke, F. Botterel, C. Cordonnier, S. Bretagne, Real-Time PCR Coupled with Automated DNA Extraction and Detection of Galactomannan Antigen in Serum by Enzyme-Linked Immunosorbent Assay for Diagnosis of Invasive Aspergillosis, J Clin Microbiol, 40 (2002) 2224-2227.

[204] N.J. Hos, P. Wiegel, J. Fischer, G. Plum, Comparative evaluation of two fully-automated real-time PCR methods for MRSA admission screening in a tertiary-care hospital, Eur J Clin Microbiol Infect Dis, 35 (2016) 1475-1478.

[205] K. Ushijima, Treatment for recurrent ovarian cancer-at first relapse, J Oncol, 2010 (2010) 497429.

[206] M. Fung-Kee-Fung, T. Oliver, L. Elit, A. Oza, H. Hirte, P. Bryson, Optimal chemotherapy treatment for women with recurrent ovarian cancer, Curr Oncol, 14 (2007) 195-208.

[207] O. Taratula, R. Savla, H. He, T. Minko, Poly(propyleneimine) dendrimers as potential siRNA delivery nanocarrier: From structure to function, Int J Nanotechnol, (2011).

[208] O. Taratula, O.B. Garbuzenko, P. Kirkpatrick, I. Pandya, R. Savla, V.P. Pozharov, H. He, T. Minko, Surface-engineered targeted PPI dendrimer for efficient intracellular and intratumoral siRNA delivery, J Control Release, 140 (2009) 284-293.

[209] J. Sapiezynski, O. Taratula, L. Rodriguez-Rodriguez, T. Minko, Precision targeted therapy of ovarian cancer, J Control Release, 243 (2016) 250-268.

[210] J.M. Hardwick, L. Soane, Multiple functions of BCL-2 family proteins, Cold Spring Harb Perspect Biol, 5 (2013).

[211] E. Abraham, A. Prat, L. Gerweck, T. Seneveratne, R. Arceci, R. Kramer, G. Guidotti, H. Cantiello, The multidrug resistance (mdr1) gene product functions as an ATP channel, Proceedings of the National Academy of Science of the USA, 90 (1993) 312-316.

[212] R. Sneath, D. Mangham, The normal structure and function of CD44 and its role in neoplasia, Mol Pathol, 51 (1998) 191-200.

[213] J. Vandooren, P. Van Den Steen, G. Opdenakker, Biochemistry and molecular biology of gelatinase B or matrix metalloproteinase-9 (MMP-9): the next decade, Crit Rev Biochem Mol Biol, 48 (2013) 222-272.

[214] L.K. Akison, R.L. Robker, The critical roles of progesterone receptor (PGR) in ovulation, oocyte developmental competence and oviductal transport in mammalian reproduction, Reprod Domest Anim, 47 Suppl 4 (2012) 288-296.